Programmed cell death in the eradication of HIV-1 infected cells by the oncolytic Maraba virus MG1

Megan Magro

Department of Biochemistry, Microbiology, and Immunology

Faculty of Medicine, University of Ottawa

Thesis submitted in partial fulfillment of the requirements for the degree of Master of Science in Microbiology and Immunology

Declaration

I, Megan E. Magro confirm that the work presented in this thesis is my own. Where information has been derived from other sources, I confirm that it has been indicated.

Date: 5th of December, 2022

Abstract

Since the start of the HIV/AIDS epidemic in 1981, 75.7 million people have become infected with HIV, and 32.7 million have died as a result. Fortunately, life-saving treatment regimens have been developed. Combination antiretroviral therapy (cART) is effective at reducing viral load to an undetectable range, thus preventing transmission of HIV. However, cART is not a cure. Latent and persistent viral reservoirs persist *in vivo,* and act as pools of infectious virus capable of re-activation if cART is abrogated. In the present work, we investigate the use of an oncolytic virus called MG1, which is capable of targeting and killing HIV infected CD4+ T cells and macrophages *in vitro*. We sought to determine the mechanism of cell death induced by MG1 to kill HIV infected cells. Our results indicate that MG1-induced cell death of HIV infected cell lines, is independent of caspases, and that caspase 3 and 7 activity is downregulated in HIV infected cell lines. We also determined that HIV infected primary monocyte-derived macrophages are preferentially killed by MG1 over the uninfected bystander cells. Ultimately, these results provide important insight towards how MG1 kills HIV infected cells *in vitro*, and together with future work, we hope to become one step closer to a potential cure for HIV.

Acknowledgements

I would firstly like to extend my greatest thanks to my supervisor Dr. Jonathan Angel for his continuous support, encouragement, and advice throughout all my years in the Angel lab. Thank you for not only helping me develop into a competent scientist, but also for the life lessons.

I would like to thank all the members of the Angel lab, past and present. Thank you to our lab technician Stephanie for her expertise and patience with me throughout graduate school. Thank you to Bengisu and former lab members Ana and Yasmeen for the laughs, coffee breaks, and true lifelong friendship.

Another big thank you goes out to my incredible parents for supporting me through every step of my studies, and always asking about my experiments even if they didn't understand what I was talking about. Thank you to my partner Weldon for being my rock and being there for me through the hard times.

Thank you to my TAC members Dr. Shawn Beug and Dr. Tommy Alain for their wonderful scientific discussion at each meeting, and for teaching me to think critically and pay attention to details.

Finally, I would like to thank the volunteers who donated blood for my project, and the Clinical Investigative Unit nurses. Without them, the macrophage work would not have been made possible.

Table of Contents

List of Abbreviations

AIDS	Acquired Immunodeficiency Syndrome
AICD	Activation-induced cell death
AM	Alveolar macrophages
ANOVA	Analysis of variance
Apaf-1	Apoptotic protease activating factor-1
Akt	Protein kinase B
ASC	Apoptosis-associated speck-like protein
AZT	Azidothymine
BcL-2	B cell lymphoma ligand 2
BHV-4	Bovine herpesvirus 4
BLT	bone/liver/thymus
BMDM	Bone marrow derived macrophages
CA	Capsid
cART	Combined antiretroviral therapy
CDC	Centres for disease control
CD4	Cluster of differentiation 4
CD8	Cluster of differentiation 8
CD32a	Cluster of differentiation 32a
CD46	Cluster of differentiation 46
CD155	Cluster of differentiation 155
CCR5	C-C chemokine receptor type 5
cIAP1/2	Cellular inhibitor of apoptosis 1/2

CPT	Camptothecin
CTL	Cytotoxic T lymphocyte
CTLA-4	Cytotoxic T lymphocyte antigen 4
CRISPR	Clustered regularly interspaced short palindromic repeats
CXCR4	C-X-C chemokine receptor type 4
DAMPs	Danger-associated molecular pattern
DC	Dendritic cell
dCA	Didehydro-cortistatin A
DISC	Death induced signalling complex
DMEM	Dulbecco's modified eagle medium
DMSO	Dimethyl sulfoxide
DNA	Deoxyribonucleic acid
eGFP	Enhanced green fluorescence protein
ELISA	Enzyme linked immunosorbent assay
FADD	Fas-associated death domain
FBS	Fetal bovine serum
FDA	Food and drug administration
GP120	Glycoprotein 120
GRID	Gay-related immune deficiency
HAART	Highly active antiretroviral therapy
HDACi	Histone deacetylase inhibitor
HIV	Human immunodeficiency virus
HPV	Human papilloma virus

HSA	Heat stable antigen
HSV-1/2	Herpesvirus type 1/2
HTLV	Human T lymphotropic virus
HVEM	Herpesvirus entry mediator
IAV	Influenza A virus
iCAD/CAD	(inhibitor) of caspase-activating DNase
IDU	Injection drug user
IFN-γ	Interferon - γ
IFN-γR2	Interferon-γ receptor 2
IFNAR1	Interferon alpha receptor 1
IL-2	Interleukin-2
IL-10	Interleukin-10
IL-1β	Interleukin-1β
IL-18	Interleukin-18
IMDM	Iscove's modified dulbecco's medium
INT	Integrase
IRES	Internal ribosome entry site
IRF3	Interferon response factor 3
ISG15	Interferon stimulated gene 15
IV	Intravenous
LRA	Latency reversal agent
LTR	Long terminal repeat
MA	Matrix

MAGE-A3	Melanoma-associated antigen A3
McL-1	Myeloid leukemia cell differentiation protein
MCMV	Murine cytomegalovirus
M-CSF	Macrophage colony stimulating factor
MDM	Monocyte derived macrophage
MeV	Measles virus
MHCI/II	Major histocompatibility complex I/II
MLKL	Mixed lineage kinase domain-like protein
MoM	Myeloid only mice
MOI	Multiplicity of infection
MSM	Men who have sex with men
NC	Nucleocapsid
NDV	Newcastle disease virus
NEJM	New England journal of medicine
NHP	Non-human primate
OV	Oncolytic virus
PAMPs	Pattern-associated molecular pattern
PBMC	Peripheral blood mononuclear cells
PBS	Phosphate buffered saline
PCD	Programmed cell death
PD-1	Programmed cell death protein 1
PLWHIV	People living with HIV
PI	Propidium iodide

PI3K	Phosphoinositide 3-kinase
PFA	Paraformaldehyde
PKC	Protein kinase C
PM	Plasma membrane
PMA	Phorbol-12-myristate-13-acetate
PR	Protease
P-TEFβ	Positive transcription elongation factor β
PVDF	Polyvinylidene fluoride
RIG-I	Retinoic acid inducible gene 1
RIPK1/3	Receptor interacting protein kinase 1/3
RNA	Ribonucleic acid
RNAP	Ribonucleic acid polymerase
RPMI-1640	Roswell parks memorial institute 1640 medium
RRE	Rev response element
RT	Reverse transcriptase
SE	Standard error
SFV	Semliki forest virus
shRNA	Short hairpin RNA
SIV	Simian immunodeficiency virus
SMAC	Second mitochondria-derived activator of caspases
STAT1/2	Signal transducer and activator of transcription 1/2
STS	Staurosporine
SV	Sindbis virus

SYK	Tyrosine protein kinase
TAA	Tumour associated antigen
TALENs	Transcription activator-like effector nucleases
TBK1	TANK binding kinase 1
TCR	T cell receptor
TLR	Toll-like receptor
TNF	Tumour necrosis factor
TNFR	Tumour necrosis factor receptor
TRADD	TNF-receptor associated death domain
TRAIL	TNF-related apoptosis reducing ligand
TRAM-1	Triggering receptor expressed on myeloid cells
UNAIDS	United nations programme on HIV/AIDS
VSV	Vesicular stomatitis virus
XIAP	X-linked inhibitor of apoptosis
ZFN	Zinc finger nucleases

List of Figures

Chapter 1: Introduction

1.1 History of HIV-1 and AIDS

The story of HIV/AIDS begins as early as the 1930's[1], however, it wasn't until the 1980's when physicians and scientists in the United States first became aware of the disease now known as HIV/AIDS[2]. In the summer of 1981, physicians in California saw an emergence of *Pneumocystis* pneumonia as well as a rare type of cancer called Kaposi's sarcoma in young gay men[3,4]. For some time, the condition was referred to as "the gay cancer" until the Centers for Disease Control (CDC) ultimately coined the condition as GRID (Gay – Related Immune Deficiency), resulting in a high degree of stigma towards the gay community.

As cases began to rise among men who have sex with men (MSM), it became apparent that the condition was also identified in injection drug users (IDU), haemophiliacs, persons of Haitian origin, and heterosexuals[5], proving the disease to infect many different types of people. By 1982, the CDC had used the term AIDS (Acquired Immune Deficiency Syndrome) to describe the disease for the first time[6].

By 1983, 35 countries around the world had confirmed cases of AIDS, and in the same year, a human T-lymphotrophic retrovirus (HTLV) believed to cause AIDS was isolated[6]. By the following year, an alarming 3,500 deaths from HIV/AIDS was reported in the USA. The year 1986 brought emergence of the new name for the virus; Human Immunodeficiency Virus (HIV)[7].

The year 1987 finally brought the first Food and Drug Administration (FDA) approved drug to treat HIV infection – the thymine analog, Azidothymine, or AZT. AZT acts as a potent

inhibitor of HIV reverse transcriptase, a crucial enzyme involved in the viral life cycle[8]. Since the approval of AZT, many other antiretrovirals were introduced, including HIV protease inhibitors (PI's), integrase inhibitors, and attachment/entry inhibitors[9]. Today, combination antiretroviral therapy (cART) is the gold standard for the treatment of HIV infection, and HIV/AIDS treatment has come a long way since 1987.

Despite improvements in HIV treatment throughout the years, and an excellent 52% reduction in global HIV infections since the peak in 1997, 1.5 million people were newly infected in 2020[10]. In 2014, the United Nations Programme on HIV/AIDS (UNAIDS) set out the 90-90-90 goal, with hopes that by 2020, 90% of people living with HIV (PLWHIV) will know their status, 90% of those who know their status will be accessing treatment, and 90% of those accessing treatment will be virally supressed[11]. Unfortunately, in 2022, we have not yet attained this goal.

Key populations of those at highest risk for HIV currently include (1) sex workers, (2) gay men and other MSM, (3) people who inject drugs, (4) women and girls, (5) transgender people, and (6) people in the prison system[11]. Many PLWHIV face challenges accessing treatment due to poverty, limited access to medical care, stigma, and gender inequalities to name a few.

Although we have come a long way since the 1980s, the global HIV/AIDS epidemic remains ongoing, and although excellent treatment such as cART does exist, the search for an HIV cure continues, and the importance of developing novel therapeutic strategies to eradicate HIV, is critical.

1.2 HIV-1 Viral Pathogenesis and Infection

1.2.1 Viral Life Cycle

HIV-1 is classified under the Baltimore classification as a class VI (+) sense single – stranded RNA virus. It belongs to the family *Retroviridae* and the genus *Lentivirus*. HIV-1 is an enveloped virus that houses a 9.75 kb genome encoding 9 viral genes, that translate into 16 viral proteins[12]. HIV Gag is an essential gene encoding structural proteins including the capsid (CA), matrix (MA), nucleocapsid (NC) and p6. HIV Pol encodes proteins essential in reverse transcription, a process unique to retroviruses whereby the RNA genome is reverse transcribed into DNA for it to be integrated into the host genome. HIV Pol encodes four proteins: reverse transcriptase (RT), protease (PR), RNaseH, and integrase (INT). The HIV Env gene encodes the viral envelope glycoproteins gp120 and gp41. Six regulatory genes are also encoding by the HIV-1 genome; Tat, Rev, Vpr, Vpu, Nef, and Vif. HIV can be divided into HIV Type 1 (HIV-1) and HIV Type 2 (HIV-2)[12]. Since this project focuses only on HIV type 1, it will be referred to hereafter as "HIV".

HIV transmission occurs through contact with infected blood, semen, or vaginal fluid, primarily through sexual contact or intra-venous (IV) drug usage with an infected individual[13]. Vertical transmission can also occur from mother to child through pregnancy, vaginal delivery, or breastfeeding[14]. The HIV lifecycle begins when the virus binds to the CD4 surface receptor of a CD4-expressing immune cell, most notably CD4+ T cells, macrophages, and dendritic cells (DC's)[15]. HIV gp120 binds to CD4, triggering a conformational change in the glycoprotein, allowing it to bind the co-receptor; CCR5 or CXCR4[16]. After binding to the co-receptor, membrane fusion occurs, allowing entry of HIV into the host cell via clathrin-mediated endocytosis[17].

The nucleocapsid undergoes partial uncoating, leaving reverse transcription to begin in the cytoplasm[12]. After RT reverse transcribes the viral ssRNA into dsDNA, HIV integrase facilitates integration of the dsDNA into the host DNA within the nucleus, forming a provirus. Proviral DNA may then be transcribed by the host RNA polymerase II resulting in unspliced RNA[18]. The first round of splicing results in the Tat, Nef, and Rev genes. After protein synthesis, Rev can facilitate nuclear export of the remaining mRNA transcripts by binding the Rev Response Element (RRE), a hairpin loop located near the 3' LTR region of the viral RNA[19]. With all required mRNA transcripts now exported from the nucleus, synthesis of HIV structural proteins can be completed by host ribosomes in the cytoplasm.

Assembly of the viral genome and nucleocapsid occurs via the accumulation of matrix (MA) proteins at the cell membrane and the recruitment of Env to form the viral envelope[20]. When the capsid structure is complete, the virus buds off with the help of Vpu which cleaves the host protein; tetherin[21].

The final step of the HIV life cycle is maturation. HIV protease (PR) cleaves the poly-proteins – Gag, Gag-Pol, and Env, finalizing the maturation of the virus and resulting in a mature virion, capable of future rounds of replication[12]. After release of the infectious progeny, new virions can infect CD4-expressing tissue resident immune cells and travel within the blood stream to other areas of the body, thereby spreading the infection systemically[22,23].

1.2.2 HIV infection and the immune system

1.2.2.1 CD4+ T cells

Since HIV targets cells of the immune system, immune dysfunction is inevitably associated with HIV infection, both at the innate and adaptive arms of the immune system. Since the primary cellular target of HIV is CD4+ T lymphocytes, one of the most notable features of HIV infection is the profound decrease in the number and function of these cells[24]. In the early stages of HIV infection, intestinal CD4+ T cells undergo rapid depletion, and thymocyte development is impaired, making it difficult to produce new cells[25,26]. CD4+ T lymphocyte abnormalities also include decreased proliferation and production of IL-2[27], downregulation of the activation ligand CD40[28], increased expression of apoptotic markers, and increase in the number of T cells undergoing apoptotic cell death[29]. Productively infected CD4+ T cells represent a small portion of the CD4+ T cell population, and bystander cell death accounts for a large portion of T cell death during HIV infection, thus contributing to the high degree of immune dysregulation[30,31].

1.2.2.2 Bystander cell death during HIV infection

Bystander cell death can occur through either (1) activation-induced cell death (AICD), (2) the effects of viral proteins released from infected cells acting on nearby cells, or (3) a combination of the two. For example, HIV gp120 has been shown to induce cell death of bystander cells via binding to the CD4 receptor[32].HIV Tat can also cause bystander cell death via uptake of Tat by neighboring cells, resulting in upregulation of caspase 8[33] and FasL[34]. HIV Nef has also been shown to induce bystander cell apoptosis via inserting into the plasma membrane (PM) of neighboring T cells and disrupting membrane homeostasis[35]. Furthermore, AICD can occur in HIV infection via HIV gp120 engagement with CD4, leading to upregulation of Fas and

FasL on the surface of the cell and thus, Fas/FasL induced apoptosis can occur[36,37]. HIV Tat has also been shown to increase FasL expression, resulting in AICD via FasL induced apoptosis[38].

1.2.2.3 CD8+ T cells

Studies using Simian Immunodeficiency Virus (SIV) infected macaques have demonstrated the importance of cytotoxic CD8+ T cells in the control of HIV infection (reviewed in [39]). Similar to CD4+ T cells, CD8+ T lymphocytes of PLWHIV also harbour functional abnormalities. CD8+ T cells have been found to have increased expression of the inhibitory marker PD-1[40], and low levels of perforin[41] suggesting T cell exhaustion, therefore making it difficult to fight off infection(s). As CD8+ T cells become exhausted, they begin to lose proliferative capacity, cytotoxic potential, and restrict the production of IL-2[42]. As CD8+ T cells become chronically exposed to viral antigen, they begin to have difficulty producing IFN-y along with other cytokines[43] and show increased susceptibility to apoptosis primarily through decreased expression of the anti-apoptotic protein; Bcl-2[44]. T regulatory cells (Tregs) can also contribute to T cell exhaustion through the production of IL-10, which inhibits T cell proliferation (reviewed in [45])

1.2.2.4 Macrophages

Unlike T lymphocytes, HIV infected macrophages harbour resistance to viral cytopathic effects[46,47], however, they do still have functional abnormalities. HIV has evolved mechanisms to prevent cell death of infected macrophages. For example, HIV Env can stimulate macrophage – colony stimulating factor (M-CSF) to downregulate tumor necrosis factor related-apoptosis

reducing ligand (TRAIL) and upregulate anti-apoptotic proteins Mcl-1 and Bcl-1, thus keeping the infected macrophage alive[48]. HIV Tat has also been shown to induce expression of Bcl-2 *in vitro*[49]. Due to their ability to resist cell death while maintaining viral infection, HIV infected macrophages serve to spread HIV throughout the body, and persist as a viral reservoir, making them a key target as a potential approach to an HIV cure.

1.3 HIV Cellular Reservoirs

1.3.1 The latent reservoir in CD4+ T cells

The term latency was first used in the clinical sense to describe the long asymptomatic period between the onset of HIV infection and the development of AIDS. It was later determined that HIV actively replicates throughout the entire course of infection, including the asymptomatic period[50]. Nevertheless, HIV can establish a state of latency, whereby the term "latency" refers to a state of dormancy, characterized by the absence of viral replication and production of virions[51,52]. Latently infected cells are present during treatment with cART, and they will "hide" from the immune system and escape immune or cART-mediated clearance.

Although cART is capable of reducing viral load to an undetectable range, the latent reservoir persists, most often in resting memory CD4+ T cells[53]. As HIV infected resting cells become activated in response to antigen, they undergo clonal expansion and a burst in cellular proliferation giving rise to effector cells. Most of these effector cells die, however a small number persist as memory cells. Latent provirus can then persist within these memory cells and escape cART-mediated clearance (reviewed in [54]). Alternatively, HIV latency can also be

established in activated CD4+ T cells, as cells become infected, most will succumb to cytopathic effects and die, however, some cells will survive long enough to revert to a memory state and establish latency[55].

Latency can be classified as pre-integration or post-integration latency, with the latter being the most common[54]. In post-integration latency, HIV DNA is first integrated into the host genome, forming a provirus. Once integration has occurred, a latent state of infection is then established. HIV latency is reversible, and *in vivo*, T cell activation is sufficient to induce latency reversal and the production of viral progeny following the cessation of cART[56].

Latently infected CD4+ T cells are quite rare in cART treated individuals, with an estimated one copy of latent provirus per 1 million CD4+ T cells[57,58]. Studies have also attempted to identify phenotypic markers of latency. One study by Descours and colleagues in 2017[59] identified CD32a as a marker of the latent reservoir, however that study was later disputed by Garcia and colleagues in 2018[60]. Thus, no markers have been successfully identified to date. These challenges have made it difficult to enrich the latent reservoir *ex vivo*, making it difficult to study. Researchers have since relied on cell line, and primary cell models of HIV latency to study the reservoir[61–63].

As mentioned, HIV latency is often established in activated CD4+ T cells as they revert to a memory state, however, there is still debate on how this state of latency is maintained within the cell. Chromatin remodelling has been proposed as a possible mechanism, whereby HIV-1 provirus is located within condensed heterochromatic regions of the DNA, something that was observed in the latently infected Jurkat derived cell line – J-Lat[64]. However, in vivo studies of

HIV integration sites later revealed that most of the HIV DNA was integrated within actively transcribed regions of the host genome[65].

DNA methylation has also been proposed as the HIV transcription start site is flanked by two CpG islands, which are methylated in both J-Lat cells, and an *in vitro* CD4+ T cell model of latency[66,67]. A few other proposed mechanisms are histone deacetylation, transcriptional interference, changes in expression of transcription factors, inhibition of RNA polymerase II elongation, and RNA splicing/export (reviewed in [54]).

1.3.2 HIV Persistence in Macrophages

In addition to the latent reservoir in CD4+ T cells, there also exists a persistent viral reservoir *in vivo.* HIV infected macrophages can harbour a persistent infection, characterized by ongoing low levels of viral replication with resistance to cytopathic effects[68].

In a 2000 study by Chun and colleagues, it was found that CD4+ T cells are not the only cell reservoir contributing to plasma viremia rebound following the cessation of HAART[69]. These results revealed that there must be existence of another HIV reservoir that can contribute to viral rebound after cessation of HAART.

A subsequent study by Aquaro et al. in 2002 examining the long-term replication and expression of HIV in macrophages *in vitro* found that macrophages survive initial infection with HIV and continue to produce virus throughout the course of infection[68]. This study ultimately concluded that CD4+ T cells represent the *latent* reservoir, whereby these cells can evade immune and drug-mediated clearance while no viral replication is occuring, and macrophages

represent the *persistent* reservoir, where they escape cell death and viral cytopathogenicities, allowing continued low levels of viral replication.

A much later 2017 study by Honeycutt et al. provided further evidence of the establishment of a persistent HIV reservoir in macrophages, *in vivo*[70]. Using humanized myeloid-only mice (MoM), the authors found that 33% of MoM had viral rebound following 7 weeks post anti-retroviral therapy (ART) cessation[70], suggesting the presence of a persistent infection in tissue-resident macrophages, and the ability of this reservoir to contribute to viral rebound if ART is interrupted.

One of the most notable features of persistently infected macrophages is their ability to resist viral cytopathic effects and cell death. This resistance to apoptosis is commonly associated with changes in expression levels of anti and pro-apoptotic proteins. Members of the B cell lymphoma 2 (BCL-2) family of proteins have been identified as key players in conferring apoptosis resistance, thus allowing HIV infected macrophages to persist within the body[71]. BCL-2 family proteins can be classified as anti-apoptotic or pro-apoptotic. A few common anti-apoptotic BCL-2 family proteins include BCL-2, BCL-XL, and MCL-1. Common pro-apoptotic proteins in this family include BAX, BAK, BAD, and BID (reviewed in [71]).

HIV replication within macrophages has been found to induce BCL-2 transcription, thus allowing cell survival[72]. Furthermore, HIV infected macrophages have been found to harbour increased expression of BCL-2 and BCL-XL, accompanied by downregulation of the pro-apoptotic proteins BAD and BAX[73]. HIV proteins Tat and gp120 have also been shown to induce expression of triggering receptor expressed on myeloid cells 1 (TREM-1) on macrophages. When TREM-1 is stimulated, this induces expression of BCL-2, leading to macrophage survival[46].

Several other proteins are also involved in HIV infected macrophage survival. Expression of cellular IAP1 (cIAP1) and cIAP2 has been found to offer protection from HIV Vpr induced apoptosis in infected monocyte-derived macrophages (MDM) and phorbol-12-myristate-13-acetate (PMA) treated THP1 cells[74]. HIV Vpr has been showed to upregulate the anti-apoptotic protein survivin, which is responsible for protecting x-linked inhibitor of apoptosis (XIAP) from proteasomal degradation, thus protecting the cell from intrinsic apoptosis[75]. **Figure 1** depicts examples of cellular proteins either upregulated or downregulated in HIV infected macrophages, thus favouring their survival.

Aside from escape from cell death, HIV persistently infected macrophages can reside in immune privileged tissues such as the brain and the genital tract and possess very long half lives ranging from ~ 2 months for alveolar macrophages[76], up to decades old in microglia[77]. Furthermore, persistently infected macrophages can also spread virus throughout the body[78]. HIV infected macrophages can recruit CD4+ T cells via release of chemotactic factors[79]. A virological synapse is then formed between MHCII and TCR, allowing the transfer of virus from one cell to another[80]. This mechanism allows transfer of viral particles and spread of the infection while evading immune or drug-mediated clearance during cART.

It is clear from the topics discussed in section 1.3, that both the latent HIV reservoir in CD4+ T cells, and the persistent HIV reservoir in macrophages serve as two *distinct* pools of virus within the body and can both contribute to viral rebound following cessation of cART. To elaborate, cART is not capable of eradicating the latent, or persistent reservoir, thus these reservoir cells are an obvious obstacle in complete elimination of HIV from the body.

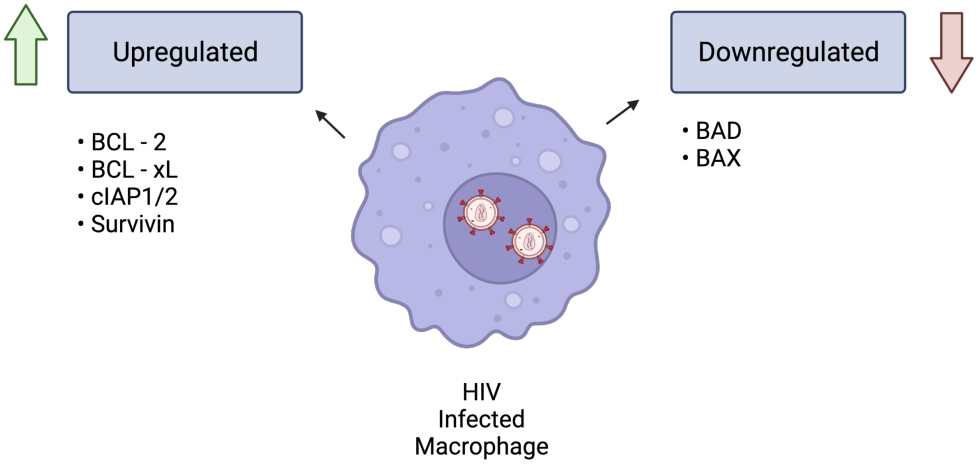
Upregulated
• BCL - 2
• BCL - xL
• cIAP1/2
• Survivin
Downregulated
• BAD
• BAX
HIV
Infected
Macrophage

Figure 1. Expression levels of proteins involved in apoptosis are altered in HIV infected macrophages, favouring their survival. Schematic made on Biorender.com

1.4 Current HIV-1 cure strategies

1.4.1 Latency Reversal

One of the most highly investigated approaches to an HIV cure is the "shock and kill" strategy. Latently infected cells are first "shocked" using a latency reversal agent (LRA) to reactivate latent provirus. Activated cells are then killed via the immune response or through viral-induced apoptosis[81]. A few common LRA's that have been identified include histone deacetylase inhibitors (HDACi), bromodomain (BRD4) inhibitors, protein kinase C (PKC) agonists, toll-like receptor (TLR) agonists, and extracellular receptor stimulants (reviewed in [81]).

Histone deacetylation causes the constriction of DNA, thus restricting gene expression and contributing to viral latency. HDACi's inhibit histone deacetylation, thus allowing viral genes to be expressed, and latency reversal[82]. One of the most researched HDACi is Vorinostat (also known as SAHA). In 2012, Archin et al. demonstrated the ability of SAHA to reactivate latent provirus *ex vivo.* Resting CD4+ T cells were isolated from 8 patients on HAART and treated with SAHA, resulting in a 4.8-fold increase in HIV RNA, leading to the conclusion that SAHA can reactivate latent provirus[83]. However, it was later identified that although SAHA is capable of viral reactivation, it does not reduce the size of the HIV reservoir[84], providing insight to the fact that a sufficient "kill" approach is still needed.

BRD4 inhibitors have been evaluated as LRA's since BRD4 has been identified as a negative regulator of HIV replication. BRD4 is a host co-factor that competes with HIV Tat to bind positive transcription elongation factor (P-TEFb), leading to increased RNA polymerase II (RNAPII) processing[81]. The inhibition of BRD4 by LRA's such as JQ1, allows Tat to bind P-TEFb,

leading to expression of HIV genes and latency reversal, which has been observed in both cell lines[85] and primary CD4+ T cells[86].

Notable other LRA's currently under investigation include PKC agonists such as Bryostatin-1, and Prostatin[87,88], TLR agonists such as Resiquimod[89] and Lefitolimod, the latter being currently under phase 2a clinical trials as an LRA (NCT02443935)[90], and extracellular receptor stimulants such as the CCR5 antagonist Maraviroc[91].

LRA's are notably useful for the reactivation of the latent reservoir, however, to develop LRA's as a potential HIV cure strategy, more research must be conducted to identify additional compounds for total eradication of the reservoir. Although many LRA's have been identified, effective "kill" agents are required to complete the "shock and kill" therapy. One such strategy is the use of therapeutic vaccines to eradicate the reservoir following reactivation. Two potential therapeutic vaccines include DC-HIV and ALVAC-HIV[92]. DC-HIV is made using dendritic cells stimulated with heat-inactivated HIV[93], while ALVAC-HIV is a canarypox vector comprising of Env, Gag, Pol, and Nef[94,95]. In a 2011 study, the DC-HIV vaccine elicited a broad T cell response against Gag, Nef, and Env and DC-HIV vaccine recipients demonstrated a decrease in viral load compared to control recipients[93]. In 2005 and 2006, ALVAC-HIV vaccine recipients showed increased CD4 and CD8 T cell responses and increase virologic control in two separate randomized control trials[94,95]. A few other possible therapeutics to eliminate the HIV reservoir include apoptosis inducers such as BcL-2 antagonists, PI3K/Akt inhibitors, and SMAC mimetics (currently under investigation by our group), as well as RIG-I inducers which activated RIG-I receptors to sense viral RNA[96].

1.4.2 Genetic Alterations

In 2009, a paper published in the New England Journal of Medicine (NEJM) by Hutter et al. gained quick popularity as it described a 40-year-old HIV+ man undergoing treatment for acute myeloid leukemia, who achieved complete viral remission in the absence of cART following a stem cell transplant from a donor who had a mutation in the CCR5 receptor[97]. Homozygosity for a 32-bp deletion in the CCR5 allele (CCR5Δ32), results in an inactive CCR5 gene. Since HIV uses CCR5 as a coreceptor for viral entry, genetic defects in CCR5 confer resistance to HIV[98]. This result was an important steppingstone in the development of using genetic alterations/gene therapy as an HIV cure strategy, however, less invasive strategies that focus on patient safety must be developed.

Further methods using genetic editing of HIV co-receptors (CCR5 and CXCR4) have been examined. Most commonly, techniques such as (1) Zinc Finger Nucleases (ZFN), (2) Transcription Activator-like effector nucleases (TALEN's), and (3) Clustered Regulatory Interspaced Short Palindromic Repeats (CRISPR/Cas9) are gaining popularity (reviewed in [99]).

ZFN's can target specific genomic sites[100], thus making them useful for the genetic editing of CCR5. A 2008 study by Perez et al. used an Adenovirus transduction method to induce ZFN-mediated modification to the CCR5 alleles of CD4+ T cells isolated from HIV-infected donors[101]. Mice engrafted with the modified cells, showed a significant reduction in viral load, compared to mice engrafted with unmodified cells[101]. A similar study conducted by Holt et al. examined the use of ZFN's in human CD34 HSPC cells, followed by transplantation of these cells in mice[102]. In this study, 17% of CCR5 alleles from HSPC's were modified, and mice transplanted with modified cells showed a significant reduction in viremia[102].

TALEN's are another gene editing technology similar to ZFN's, although some studies have shown that TALEN's are less cytotoxic than ZFN's[103,104]. In 2018, engineered TALEN's were used to generate the CCR5Δ32 mutation in an in vitro model, using CD4+ U87 cells[105]. However, CRSIPR/Cas9 gene editing technology has been shown even more effective than ZFN's or TALEN's[103].

When TALEN's were compared with CRISPR technology, it was found that CRISPR was more than twice as effective at generating the CCR5Δ32 mutation in induced pluripotent stem cells (iPSC's) than TALEN's[106]. Furthermore, CRISPR/Cas9 technology was capable of excising pro-viral DNA from patient immune cell engrafts in humanized mice[107]. CRISPR is certainly a current leader in gene editing technology, with a very recent study (April 2022) identifying host genes that alter HIV infection (including Vif and Tat binding factors), with the goal of examining the effects of CRISPR/Cas9 knock-out of these genes and their implications as a possible HIV cure strategy[108].

1.4.3 Block and Lock

Due to the many challenges in attaining an HIV cure via full elimination of HIV from the body, the block and lock strategy has been investigated as a functional cure for HIV, whereby transcription of latently infected cells is silenced, and reactivation is prevented.

Various potential block and lock strategies have been investigated, most of them targeting proteins involved in viral transcription. One of the most studied block/lock strategies is the use of Didehydro-Cortistatin A (dCA) as an HIV Tat inhibitor[109]. Since HIV Tat is responsible for transcription elongation, it is a suitable target for inhibition[110]. dCA has been shown to block

HIV transcription and reactivation in cell lines, primary CD4+ T cells, and humanised bone marrow/liver/thymus (BLT) mice[111–113], proving to be a promising candidate to employ the block and lock strategy.

Another potential candidate is a class of integrase inhibitors called LEDGINs. LEDGINs inhibit HIV integration into the host DNA and enhance integrase oligomerization resulting in defective viral progeny[114–116]. Although still in the early stages, in 2018 Debyser and colleagues postulated based on previous data that LEDGINs can inhibit viral integration and target residual proviruses to sites that are less susceptible to reactivation[117]. Although a potential pitfall in the use of LEDGINs may be that they must be administered immediately following acute infection with HIV in order to affect reservoir formation, and it is currently unknown whether they would have an effect in patients chronically infected.

Short hairpin RNA (shRNA) has also been investigated as a block/lock strategy. Two shRNA's called 143 and Prom A were investigated by Kelleher, Suzuki, and colleagues, both of which target transcription factor binding sites in the long terminal repeat (LTR) promotor region[118,119]. These shRNA act to silence HIV transcription via recruiting histone modifiers which promote chromatin remodeling resulting in heterochromatin[119]. Both 143 and Prom A have been successful at reducing reactivation when treated with LRA's in the latently infected Jurkat cell line, J-Lat[119].

1.5 Oncolytic Viruses – a potential HIV cure strategy

1.5.1 Introduction to oncolytic viruses – the cancer field

Oncolytic viruses (OV's) have recently emerged as an immunotherapeutic agent for the treatment of various cancers. OV's are viruses that can target and kill tumor cells, while sparing the healthy cells[120]. Most often, OV's are genetically modified versions of a naturally occurring virus to enhance the oncolytic effects, improve selectivity for tumor cells, or attenuate the virus in healthy cells. To date, many OV's have been tested *in vitro* and in clinical trials, with four OV's currently approved globally (reviewed in [121]).

In 2004, the first OV - a Picornavirus called Rigvir was approved for the treatment of Melanoma, however, it never achieved widespread use[122]. The following year, a genetically modified Adenovirus called Oncorine (H101) was approved in China for the treatment of head and neck cancers[123]. To follow suit was T-VEC and DELYTACT, both genetically modified herpes simplex viruses (HSV-1) used to treat metastatic melanoma, and primary brain cancers, respectfully[124,125].

Both DNA and RNA viruses are being investigated as potential OV's. DNA viruses have the advantage of high genomic stability, while RNA viruses are often highly immunogenic[126–128]. Oncolytic DNA viruses include Adenovirus, Herpes simplex virus 1 and 2 (HSV-1, HSV-2), Parvovirus, and Poxvirus. Oncolytic RNA viruses include a wider range of candidates, including Semiliki forest virus (SFV), Sindbis virus (SV), Zika virus, Newcastle disease virus (NDV), Measles virus, Coxsackie virus, Poliovirus, Seneca valley virus, Vesicular Stomatitis virus (VSV), and Maraba virus (reviewed in [121]).

OV's exploit cancer cell specific characteristics in order to target and infect tumour cells. For example, cancerous cells often overexpress certain cell surface receptors such as CD46, CD155, or integrin $\alpha 2\beta 1$ - which serve as attachment/entry receptors for measles virus,

poliovirus, and echovirus, respectfully[129–131], allowing OV's engineered from these viruses to primarily infect cancer cells. HSV derived OV's rely on the overexpression of herpesvirus entry mediator (HVEM) on cancer cells for viral entry[132].

OV's can also exploit intracellular signalling defects to preferentially infect tumour cells. Cancer cells often have defects in anti-viral signalling, particularly, type I and II interferons (IFN)[133]. Some examples of OV's known to exploit these defects in IFN signalling are Measles virus (MeV)[134], VSV[135], and Maraba virus[136].

1.5.2 The genetically engineered Maraba virus – MG1

Maraba virus is a (-)ssRNA virus belonging to the family *Rhabdoviridae*[137]. As mentioned in section 1.5.1, Maraba virus is an oncolytic virus capable of targeting cancer cells due to impairment in the antiviral IFN signalling cascade[136]. Maraba virus exploits these defects to kill tumour cells, while leaving the healthy cells untouched.

VSV, a close relative of Maraba virus, has also been identified as an oncolytic virus that exploits IFN signalling defects in cancer cells[138,139]. VSV has been genetically edited (removal of Methionine-51 from the M protein) to harbor increased sensitivity to IFN-defective tumours, leading to the VSV variant VSVΔ51[135]. To follow suit, J. Brun and colleagues introduced a series of genetic edits in Maraba virus and screened its oncolytic potential against a series of tumour cell lines. A double mutant Maraba virus containing amino acid substitutions in the M protein (L123W), and G protein (Q242R) was a potent oncolytic virus, demonstrating enhanced oncolytic potential in tumour cells, and greater attenuation in healthy cells compared to its cousin, VSVΔ51[136]. This Maraba virus mutant was termed MG1.

These genetic mutations aid to (1) attenuate MG1 in healthy cells, and (2) further prevent MG1 from antagonizing the host IFN response[114]. The matrix (M) protein mutation contributes to MG1 attenuation in healthy cells and prevents the virus from interfering with host IFN production, as PC3 tumour cells continued to produce IFN when infected with the M mutant virus (L123W), and double mutant (MG1) as observed by J. Brun and colleagues[114]. The glycoprotein (G) mutation also contributes to attenuation of MG1 in an *in vivo* xenograft tumour model in mice[114].

Since the original identification of MG1 as a potent oncolytic virus in 2010, many studies have followed with the goal of developing MG1 for clinical use as an oncolytic virotherapy. M.J Atherton and colleagues investigated an MG1 based vaccine for the treatment of Human Papilloma Virus (HPV)-associated cancers (MG1-E6E7) in mice and found that vaccination with MG1-E6E7 cleared large tumours in a CD8+ - dependent manner[140]. MG1 in combination with Paclitaxel has also been identified as a successful treatment for breast cancer in mice[141].

MG1 safety has also been investigated in cats, with limited side effects observed[142], and a prime:boost vaccination strategy using an Adenoviral vaccine aimed at priming the immune system against a tumour-associated antigen (TAA), followed by an MG1 based vaccine targeting the same TAA was examined in non-human primates (NHP's). This vaccine termed Ad:MG1 expresses the melanoma-associated antigen A3 (MAGE-A3) and was found to have no adverse effects in NHP's. It has since entered clinical trials for the treatment of solid tumours (NCT02285816, NCT02879760)[143].

1.5.3 MG1 and HIV infection

Like tumour cells, HIV infected cells including latently infected CD4+ T cells and persistently infected macrophages harbour impaired IFN signalling, including inhibition of interferon response factor 3 (IRF3) by Vpr[144], proteasomal degradation of retinoic acid inducible gene-I (RIG-I) by HIV protease[145], impairment of protein kinase RNA - activated (PKR) by Tat[146], and downregulation of major histocompatibility complex 1 (MHC-1) by Nef[147].

Due to the presence of IFN signalling defects in HIV infected cells, we have identified that, like in cancer studies, MG1 can target and kill HIV infected cells while sparing the healthy bystanders. Our group has verified the ability of MG1 to target/kill HIV infected cells in a wide range of *in vitro* models, including HIV latently infected cell lines - U1 and OM10.1[148], an *in vitro* model of latency using primary CD4+ T cells[125], alveolar macrophages derived from bronchiolar fluid[126], and a monocyte-derived macrophage model[149].

Very recently, our group has also begun studies of MG1 *in vivo* using a humanised mouse model (in progress). This work has kickstarted the development of MG1 as a potential curative therapy for HIV infection. However, more research is needed before MG1 can possibly be used in a clinical setting. Although we have identified an ability of MG1 to kill HIV infected cells, the mechanism by which MG1 induces cell death is yet to be elucidated. This knowledge is crucial information to provide insight on the development of MG1 for clinical use.

1.6 Programmed cell death (PCD)

Programmed cell death (PCD), particularly apoptosis was first discovered in 1972 by Kerr and colleagues[150]. Since then, there have been many advances in the field of cell death. Currently, numerous cell death pathways exist, including caspase-dependent, and caspase-

independent pathways. Caspases are a group of endoproteases, responsible for carrying out many cell death pathways once they are cleaved into their active form[151]. Some caspase-dependent pathways include apoptosis, and pyroptosis, and caspase-independent PCD includes necroptosis.

1.6.1 Caspase – dependent cell death

1.6.1.1 Apoptosis

Many viruses have been shown to induce programmed cell death pathways in their infected cells to propagate/release infectious viral particles, allowing for viral egress and disease progression. Apoptosis is the most widely known mechanism of programmed cell death, whereby "programmed" refers to an active process that relies on a change in gene expression[150]. Programmed cell death differs from necrotic cell death, as necrosis is a passive process occurring due to cell damage[150].

Two primary apoptotic pathways exist; extrinsic and intrinsic. Both pathways rely on the activation of caspase proteins, a large family of cysteine proteases that act in cascades[152]. The extrinsic pathway involves binding of a ligand to a death receptor such as TNF/TNFR, FAS/FASL, or TRAIL/TRAILR. Upon ligand binding, clustering of the cytoplasmic domains of the receptor occurs, and adaptor proteins such as fas-associated death domain (FADD) or TNF-receptor associated death domain (TRADD) are recruited. Formation of the death-induced signalling complex (DISC) occurs via the association of FADD/TRADD with pro-caspase 8, after which auto-catalytic activation of pro-caspase 8 into caspase 8 is carried out. Caspase 8 is released into the

cytosol to activate the executioner caspase 3 (reviewed in [153]). One common example of extrinsic apoptosis is perforin/granzyme - mediated killing by cytotoxic T lymphocytes (CTL's)[154].

Intrinsic apoptosis is mitochondrial- dependent and is triggered via cell stress such as hypoxia, toxins, or radiation[153]. It involves the release of cytochrome C from the mitochondria due to the activation of pro-apoptotic proteins of the Bcl-2 family (ex: Bax and Bad). Cytochrome C binds to and induces a conformational change in apoptotic protease activating factor-1 (Apaf-1) which induces the formation of the apoptosome. The apoptosome recruits and activates pro-caspase 9 and pro-caspase 3 into their active forms, whereby caspase-9 activates downstream effector caspases and caspase 3 cleaves inhibitor of caspase-activating DNase (iCAD) into CAD. CAD then causes DNA fragmentation and advanced chromatin condensation leading to cell death[155]. Ebola virus has been shown to induce extrinsic apoptosis, while Influenza A virus and HIV have been shown to demonstrate intrinsic apoptosis [156–158].

1.6.1.2 Pyroptosis

Another widely studied mechanism of programmed cell death is pyroptosis. Pyroptosis is a pro-inflammatory process characterized by excessive inflammation and occasional development of cytokine storms and inflammatory tissue damage *in vivo* (reviewed in [159]).

Pyroptotic cell death involves the activation of inflammasomes by pathogen and/or danger associated molecular patterns (PAMP's/DAMP's). Inflammasomes – such as NLR pyrin family domain containing 3 (NLRP3), are multi-protein complexes that mediate the activation of pro- caspase 1 into its active form[160]. Inflammasomes sense PAMP's/DAMP's released from dying cells, which in turn allows for the cleavage of pro-caspase 1 into caspase -1 via the

association of apoptosis-associated speck like protein (ASC) to the inflammasome complex[161]. Caspase-1 cleaves pro-IL-1β and pro-IL-18 into their active forms (IL-1β and IL-18), as well as cleaves a pore forming protein called gasdermin D. Active gasdermin D travels to the plasma membrane where it forms a pore, allowing for the release of IL-1β and IL-18, loss of cell membrane integrity and homeostasis, ultimately resulting in cell death and a pro-inflammatory state[162].

Many RNA viruses have been shown to activate pyroptosis, including Rabies virus, Hepatitis C virus, and Influenza virus[163–165].

1.6.2 Caspase – independent cell death

1.6.2.1 Necroptosis

Necroptosis is one of the most studied caspase-independent cell death processes. It is a type of programmed cell death that is mediated by receptor interacting protein kinases 1 and 3 (RIPK1/3) and mixed lineage kinase domain-like protein (MLKL)[166,167]. Typically, necroptosis requires the inhibition of caspases, particularly caspase 8[168,169]. Caspase 8 generally inhibits RIPK1, thus allowing the cell to undergo apoptosis. However, if caspase 8 is absent or inhibited - such as through the action of viral proteins, RIPK1 becomes activated, and the cell undergoes necroptosis[170]. Caspase 8 can thus be seen as a molecular switch, dictating whether the cell will undergo apoptosis or necroptosis.

Like apoptosis, necroptosis is initiated through binding of a ligand to a death receptor such as TNF/TNFR, TRAIL/TRAILR, or FAS/FASL[170]. This binding recruits RIPK1/3 to the

cytoplasmic domain of TNFR, forming a complex called the necrosome[171]. Activated RIPK3 phosphorylates MLKL, allowing MLKL to translocate to the plasma membrane and disrupt membrane integrity, leading to death of the cell[172]. Necroptosis is a pro-inflammatory process that involves the release of DAMPs from the cell, unlike apoptosis which is anti-inflammatory. Noteworthy viruses that are known to induce necroptosis are HIV[173] and vaccinia virus[174].

A visual comparison of the mechanisms of apoptosis, necroptosis, and pyroptosis can be seen in **Figure 2.**

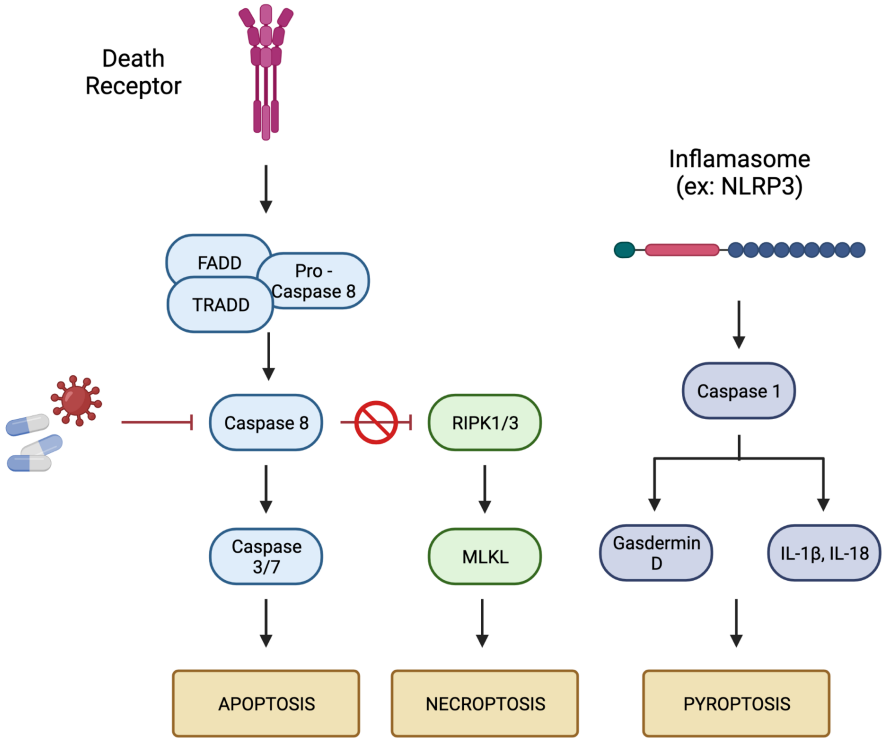
Death
Receptor
FADD
TRADD
Pro -
Caspase 8
Caspase 8
Caspase
3/7
APOPTOSIS
RIPK1/3
MLKL
NECROPTOSIS
Inflamasome
(ex: NLRP3)
Caspase 1
Gasdermin
D
IL-1β, IL-18
PYROPTOSIS

Figure 2. Comparison of the molecular mechanisms of extrinsic apoptosis, necroptosis, and pyroptosis. Schematic made on Biorender.com

1.7 Project Rationale/Significance

HIV treatment and cure research has made tremendous advancements since the start of the HIV epidemic in the 1980s. cART is the gold standard in the treatment of HIV infection, and it effectively reduces viral load to levels that are undetectable. However, cART is a lifelong treatment and not a cure. HIV latently infected CD4+ T cells and persistently infected macrophages serve as reservoirs of infectious virus, resulting in viral rebound if cART is interrupted. HIV cure research is highly focused on the complete eradication of these reservoirs, and oncolytic virotherapy is certainly a candidate to achieve this goal.

We have shown that the OV MG1 can target and kill HIV infected CD4+ T cells and macrophages *in vitro*. However, the mechanism of cell death induced by MG1 is yet to be elucidated. This project examines programmed cell death pathways during MG1 infection, with the hope of gaining insight towards how MG1 is capable of killing HIV infected cells, in order to apply this knowledge to the development of MG1 for clinical use.

1.8 Hypothesis

The hypothesis of this work is that MG1 employs a programmed cell death pathway(s) to initiate the killing of (1) HIV latently infected CD4+ T cells, and (2) HIV persistently infected macrophages.

1.9 Project Aims

This project has two aims, which are listed below.

Investigate programmed cell death pathways as possible mechanisms for MG1 – mediated killing of;

1. HIV infected cell lines
    1.1 Myelocytic cell lines
    1.2 Lymphocytic cell lines
2. HIV infected primary monocyte-derived macrophages (MDM)

Chapter 2: Materials and Methods

2.1 Tissue culture of cell lines

Jurkat (ATCC #: TIB- 152), HL60 (ATCC #: CCL - 240), Vero (ATCC #: CCL - 81), and HEK293T (ATCC # CRL - 3216) cell lines were obtained from American Type Culture Collection (ATCC, Manassas VA). J1.1 (NIH # ARP – 1340) and OM10.1 (NIH # ARP – 1319) cell lines were obtained through the NIH AIDS Reagents Program, OM10.1 cells courtesy of Dr. Salvatore Butera[175] and J1.1 cells from Dr. Thomas Folks.[176] Vero and HEK293T cells were cultured in Gibco® Dulbecco's Modified Eagle medium (DMEM), and HL60 were cultured in Gibco® Iscove's Modified Dulbecco's medium (IMDM). DMEM was supplemented with 10% fetal bovine serum (FBS), and IMDM was supplemented with 20% FBS. Both media stocks were supplemented with 100 units(U)/ml penicillin/streptomycin (PenStrep, ThermoFisher Scientific), and 2mM L – Glutamine (ThermoFisher Scientific). Cells were grown in T75 flask (Falcon™, Thermo Fisher Scientific) and routinely split every 2 days to maintain the monolayer. TrypLe

(Gibco®, ThermoFisher # 12604013) was used to detach and re – seed adherent cell lines (Vero, HEK293T) at approximately $2x10^5$ cells/ml in a total volume of 10ml. Jurkat, J1.1, and OM10.1 cells were cultured in Gibco® Roswell Park Memorial Institute 1640 medium (RPMI-1640, ThermoFisher) supplemented with 10% FBS, 100U/ml PenSrep, and 2mM L-Glutamine. Cells were maintained at 0.5-1 $x10^6$ cells/ml with routine splitting. Healthy pro-monocytic U937 and HIV infected U1 cells were used for supplementary experiments (**Supplementary figures 3, 4, and 5**). Both cell lines were maintained in RPMI-1640 with 10% FBS, 100U/ml PenStrep, and 2mM L-Glutamine.

2.2 Amplification of oncolytic virus

The eGFP-expressing recombinant oncolytic virus MG1 was obtained from Dr. John Bell at the Ottawa Hospital Research Institute and propagated as previously described[136,138]. Briefly, approximately 10 x 10^6 Vero cells were plated in 3 T75 flasks in DMEM supplemented with 10% FBS, 100units(U)/ml PenStrep, and L-Glutamine. Cells were incubated overnight (O/N) at 37° C with 5% CO_2. The next day, MG1 was diluted in serum (FBS)-free DMEM to obtain an MOI of 0.05. Media was removed from each flask, and 1ml of virus/media mixture was added dropwise to the cell monolayer. Cells were incubated at 37° C with 5% CO_2 for 45 minutes, turning the plate every 15 minutes for optimal virus spreading. After incubation, media was topped up to 10ml with DMEM + 2% FBS and cells were incubated for 24 hours.

The following day, cell supernatants were harvested and centrifuged at 1400 rpm for 10 minutes to pellet any debris (Hereaus Instruments, Megafuge 1.0). The supernatants were

filtered through a 0.2um bottle top filter (Nalgene®, Millipore-Sigma #Z358223) and virus was pelleted at 14,000 rpm for 90 minutes at 4° C (Beckman Coulter, Avanti JXN-26). The virus pellet was resuspended in Phosphate Buffered Saline (PBS) and aliquoted into 10ul aliquots and stored at -80° C.

2.2.1 Titer by plaque assay

MG1 titer was determined through standard plaque assay. Vero cells were seeded in a 6-well plate (Corning®) at $1x10^6$ cells per well in DMEM supplemented with 10% FBS, PenStrep, and L-Glutamine and left to incubate O/N at 37° C with 5% CO_2. After 24 hours, media was removed from the wells and replaced with serial dilutions of MG1/media starting at a dilution of $1x10^7$ and ending with a dilution of $0.5x10^9$. Two wells with PBS instead of virus were also included (mock). The plates were incubated for 45 minutes, after which a 1:1 mixture of 1% agarose (Sigma-Aldrich #A5093) + 2x DMEM was added to the wells and allowed to solidify at room temperature (RT). Following a 24-hour incubation at 37° C, plaques were visualized and counted using crystal violet staining. MOI was calculated by averaging the number of plaques per well and multiplying with the dilution factor then dividing by volume.

2.3 OV infection

For MG1 dose-response experiments, Jurkat/J1.1 and HL60/OM10.1 cells were infected with MG1 at MOI 10^{-5} to MOI 1. Briefly, cells were plated in 12 well plates (Corning®) at $5x10^5$ cells/ml in RPMI media (except for HL60 which were plated in IMDM) with supplements listed in

section 2.1. 10-fold serial dilutions of MG1 were prepared in media to obtain the desired MOI for infection, and infection was performed by adding 100ul of virus to each well, excluding the mock. Infected cells were incubated for 24 hours at 37° C with 5% CO_2. At 24hpi, cells were prepared for staining and infection/cell death was analyzed using flow cytometry. Experiments were also performed on healthy pro-monocytic U937 vs. HIV infected U1 cells (**Supplementary figure 3**). The gating strategy used is shown in **supplementary figure 2**.

2.4 Treatment with caspase inhibitors and cell death inducers

For cell death experiments, two caspase inhibitors were used, (1) the pan-caspase inhibitor Z-VAD-FMK (R&D Systems, FMK001) and (2) the caspase 3 inhibitor Z-DEVD-FMK (R&D Systems, FMK004). Both caspase inhibitors were optimised in all cell lines prior to experiments (**Supplementary figures 6, 7, and 8**) and inhibitors were proven to be non-cytotoxic (**Supplementary figure 10**). Jurkat, J1.1, and OM10.1 cells were plated in a 12 well plate at $5x10^5$ cells/ml in RPMI-1640 media. Cells were pre-treated for 1 hour with 50uM of either Z-VAD-FMK or Z-DEVD-FMK at 37° C. After the 1-hour pre-incubation, cells were infected with MG1 at MOI 10^{-4}, 10^{-3}, 10^{-2}, or left uninfected. The MOI to use for infection was optimised by performing MG1 dose response experiments (**Figures 4, 5 and supplementary figure 3**). Infection was performed by adding 100ul of virus/media mixture to the well, as described in section 2.3. As positive controls, three wells were treated with the following: well 1; the chemical cell death inducer Staurosporine (Jurkat, J1.1, Sigma-Aldrich # S6942) or Camptothecin (OM10.1, Sigma-Aldrich # PHL89593), well 2; either cell death inducer + Z-VAD-FMK, or well 3; either cell death inducer + Z-DEVD-FMK. The concentration of chemical cell death inducer to

use was optimized on each cell line (**Supplementary figure 9**). A DMSO (Sigma-Aldrich # 472301) vehicle control was also included as both caspase inhibitors are dissolved in DMSO. Plates were incubated for 24 hours at 37° C with 5% CO_2, after which cells were stained with two cell death stains (described in section 2.5) and analyzed using flow cytometry. Gating strategy is shown in **supplementary figure 1**. Experiments were also performed on healthy U937 cells (**Supplementary figure 4**). Schematic representation of this methodology is shown in **figure 3.**

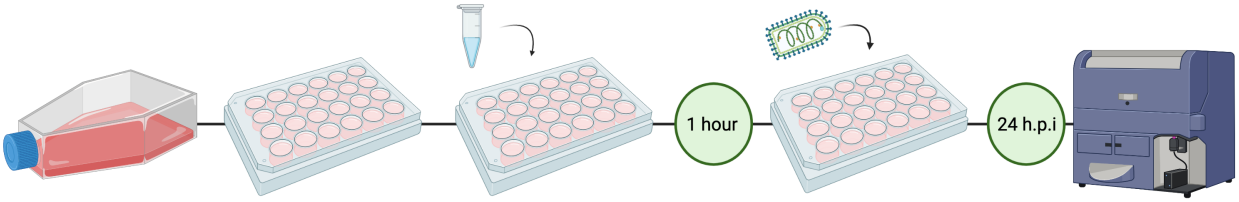

Plate cells @ 5 x10^5 cells/ml

Pre-treat with cell death inhibitor

MG1 infection

AnnexinV/PI staining for FC

Figure 3. Methodology used for cell death experiments involving treatment with caspase inhibitors during MG1 infection. Schematic made on Biorender.com

2.5 Flow cytometry of cell lines

2.5.1 eGFP and cell death staining

For MG1 dose response experiments, Propidium Iodide (PI, Biolegend # 421301) staining was used. PI binds cellular DNA present after cell death, thus cells that are PI+ are considered dead cells. $2.5x10^5$ cells were collected into 5ml polypropylene tubes (Falcon™, ThermoFisher Scientific) and pelleted via centrifugation by spinning at 1600 rpm for 5 minutes. Cells were washed once with PBS and spun again at 1600 rpm for 5 minutes. PI stain was mixed with PBS at a ratio of 0.1ul PI : 300ul PBS, and cells were resuspended in 300ul of the PI:PBS mixture and left to incubate for 5 minutes at RT in the dark. Cells were then fixed with 100ul cold 4% paraformaldehyde (PFA) for 15 minutes in the dark at RT. Cell death and infection (based on eGFP expression) was analyzed using the Beckman Coulter CytoFLEX flow cytometer, reading on FITC and ECD channels. Since MG1 – infected cells producing eGFP protein upon infection with the recombinant virus, infection can be analyzed using eGFP expression.

For cell death experiments using caspase inhibitors, AnnexinV/PI staining kit (Abcam # ab214484) was used. $1x10^5$ cells were collected into 5ml polypropylene tubes (Falcon™) and washed twice with PBS by centrifuging at 1600 rpm for 5 minutes. Cells were then resuspended in 100ul of AnnexinV binding buffer (Abcam, # ab14084), and 5ul of AnnexinV stain and/or 5ul of PI stain was added to each tube (excluding the unstained control). Tubes were incubated for 15 minutes at RT in the dark and then subsequently fixed in 4% cold PFA. Cell death was once again analyzed on the Beckman Coulter CytoFLEX flow cytometer, reading for AnnexinV (APC), PI (ECD), and eGFP (FITC). Gating strategy for data analysis is shown in **supplementary figure 1**.

2.5.2 Caspase 3 and 7 staining

To examine caspase activity during MG1 infection, a caspase 3/7 stain for flow cytometry called FLICA 660 (Immunochemistry Technologies, #9125) was used. FLICA 660 fluorescently labels active caspase 3 and 7 in living cells via labelling the aspartate-glutamate-valine-aspartate (DEVD) sequence in caspases. Jurkat, J1.1, and OM10.1 cells were plated at $5x10^5$ cells/ml in 12 well plates and infected with MG1 at MOI 10^{-2}, as previously described. Cells were left to incubate O/N at 37° C with 5% CO_2. The next day, 295ul of cells/media was added to 5ml polypropylene tubes. FLICA 660 stain was diluted 1:5 in PBS and 5ul of stain was added to each tube (1:60). Tubes were then incubated at 37° C for 1 hour. After the incubation, cells were washed 3 times in 1x apoptosis buffer (Immunochemistry Technologies, # 635) by centrifuging at 1600 rpm for 5 minutes. After the third wash, cells were resuspended in 300ul PBS and fixed with 100ul of 4% PFA (incubated for 15 minutes at RT in the dark). Cells were analyzed on flow cytometry. Experiments were also repeated on the healthy pro-monocytic U937 cells (**Supplementary figure 5**).

2.6 Production of HIV-1 stocks

The HIV NL4.3 BAL IRES HSA plasmid encoding the CCR5 (R5) tropic virus was obtained from Dr. Michel J Tremblay at the Université de Laval. The virus was amplified on HEK293T cells as follows. $2x10^6$ cells/T75 flask were seeded and incubated overnight to allow the monolayer to form. Transfection was performed using Lipofectamine™ 2000 (ThermoFisher™) and OptiMEM™ I reduced serum media (Gibco® from ThermoFisher™) with 20ug of plasmid per

flask. Mock infected controls were also transfected with an equivalent volume of PBS in replace of plasmid. 1.5ml of Lipofectamine™/OptiMEM™ and plasmid or PBS mixture was added to the cell monolayer, and fresh DMEM was added to top up the total volume to 10ml. Cells were incubated for 48 hours at 37° C with 5% CO_2, after which the supernatants were collected and centrifuged at 1600 rpm for 5 minutes. Supernatants were collected and filtered twice, firstly through 0.45um polyvinylidene (PVDF) filters and secondly through 0.22um PVDF filters (CellTreat Scientific Products). Virus stocks were aliquoted into cryovials and frozen at -80° C.

HIV titer was determined by p24 ELISA Antigen Capture Kit (Frederick National Laboratory for Cancer Research, Frederick MD, NIH AIDS Reagents Program), following the manufacturer's instructions. Briefly, the virus stock was serial diluted in sample diluent and ran in duplicate in a 96 well plate simultaneously to 8 serial dilutions of HIV-1 p24 standard (HPLC purified-HIV-1 CL.4/H9 p24 from AIDS Reagents) also run-in duplicate to create a standard curve. The plate was coated with murine purified IgG antibody (AIDS Reagents, Lot: PP292-3) before the addition of standards and virus sample. Primary antibody used was Rabbit anti-HIV p24 (AIDS Reagents, Lot: SP2143A), secondary antibody was the HRP conjugated goat anti-rabbit IgG (AIDS Reagents, Lot: 074-1516). Standard curve was made using Graph Pad Prism software. Unknowns were extrapolated from the standard curve and multiplied by the dilution factor to obtain the concentration of p24.

2.7 Isolation of peripheral blood mononuclear cells (PBMC)

Experiments relying on the participation of healthy volunteers were approved by The Ottawa Health Science Network Research Ethics Board. Healthy volunteers provided written consent to partake in the study.

PBMC were isolated from whole blood of healthy donors via density gradient separation. Blood was first collected by venipuncture in 60ml heparin (LEO Pharma Inc. Thornhill ON) containing syringes using venipuncture, after which 30ml of blood was overlay onto 20ml of Lymphoprep (StemCell Technologies, Vancouver, British Colombia Canada) and centrifuged at 1600 rpm for 30 minutes with no brake (Heraeus Instruments Megafuge 1.0). The buffy coat was collected and added to fresh 50ml conical tubes (Falcon^{TM}, Thermo Fisher Scientific) and cells were centrifuged at 1200 rpm for 20 minutes with the centrifuge brake in the on position. Cells were washed twice in PBS, and then resuspended in 10ml PBS/syringe of blood for cell counting using a hemocytometer. Cells were centrifuged once more at 1600 rpm for 10 minutes and resuspended in serum-free RPMI-1640 to proceed to monocyte isolation.

2.8 Generation of monocyte-derived macrophages (MDM)

Monocytes were separated from healthy donor PBMC via plate adherence. PBMC were resuspended in warm serum-free RPMI-1640 supplemented with PenStrep and L-Glutamine. PBMC were seeded at $3x10^6$ cells/ml in 12 well tissue culture plates (Corning®) and left to adhere for 2 hours at 37° C. After the 2-hour incubation, non-adherent cells were removed by washing the plates with warm endotoxin-free PBS (Sigma-Aldrich), after which 1ml/well of

warm RPMI-1640 supplemented with 10% heat inactivated human AB serum, PenStrep, L-Glutamine (Mϕ media) and 25ng/ml of macrophage-colony stimulating factor (M-CSF, BioLegend # 574802) was added. Cells were incubated at 37° C for 7 days with a wash and a Mϕ media replacement at day 4. On day 7, macrophages were washed with warm endotoxin-free PBS and were ready for HIV infection.

2.9 HIV Infection of MDM

At 7 days post PBMC isolation, MDM were washed with warm endotoxin-free PBS and cells were infected with 100ng of HIV in 500ul of Mϕ media. Cells were incubated for 24 hours, and media was topped up to 1ml the following day. Cells were infected for 6 days at 37° C with a wash in PBS and media replacement on day 3.

2.10 MG1 infection of MDM

At 6 days post infection (d.p.i), MDM were infected with MG1 at MOI 1, 5, or 10. Serial dilutions (2x) of MG1 were made in Mϕ media and 100ul of each dilution was added to the appropriate well. Infected MDM were then incubated at 37 ° C for 24 hours.

2.11 Flow cytometry of MDM

At 24 h.p.i with MG1, HIV infected MDM were prepared for staining by detaching the cells with warm Accutase (Millipore-Sigma) for 30 minutes at 37° C and vigorous pipetting followed by aliquoting cells into 5ml polypropylene tubes ($5x10^5$ cells per tube). MDM were

then stained with AnnexinV (Biolegend, cat #: 640907) and APC-conjugated anti-heat stable antigen (HSA) antibody (Biolegend, cat #: 101813) as previously described[149]. Since HIV BAL IRES HSA encodes murine HSA, HIV infected cells will express HSA as a surface marker allowing the HIV infected cells to be labelled as HSA+ and the HIV uninfected cells as HSA-. This method allows us to distinguish between the HIV+ (I.e HSA+) and HIV- (HSA-) populations. To analyze cell death, flow cytometry was performed analyzing eGFP expression, HSA expression, and AnnexinV. Gating strategy is shown in **Figure 11A.**

2.12 p24 ELISA

HIV p24 antigen concentration was measured on cell lines and primary MDM using the p24 Antigen Capture Kit (Frederick National Laboratory for Cancer Research, Frederick, MD. NIH AIDS Reagents Program) according to the manufacturer's protocol and as previously described in *Section 2.6*. On MDM, HIV p24 antigen concentration was measured 6 d.p.i with HIV in order to optimise how much HIV to use for infection (**Supplementary figure 11**). On J1.1 and OM10.1 cell lines, p24 antigen concentration was measured following re-activation with TNF-α in order to confirm latency (**Supplementary figure 12**). Cell-free supernatants were lysed for 1 hour at 37° C using 1% Triton-X and absorbance was read at 450nm and 650nm using the Multiskan Ascent 96 plate Reader. Standard curves were made using GraphPad Prism 9.2.0 software and p24 antigen concentration (ng/ml) was interpolated from the standard curve.

2.13 Analysis, Statistics, and Artwork

All flow cytometry data was analyzed using FlowJo™ v10.0 software. All graphs and statistics were calculated using Graph Pad Prism 9.2.0 software. Where necessary, the following statistics were run, a two-way ANOVA with multiple comparisons, paired student's T tests, one-way ANOVA, or linear regression analysis. In each case, p-values < 0.05 were considered significant (*). ** = p-value < 0.01, *** = p-value < 0.001, and **** = p-value < 0.0001. Unless otherwise cited, all schematics were made using BioRender.com.

Chapter 3: Results

3.1 HIV infected and uninfected cell lines are permissible to MG1 infection and undergo cell death during infection

To verify that MG1 preferentially infects and kills HIV infected cell lines, two pairs of HIV uninfected parental cell lines and their HIV infected counterpart were used. HL60 (parent) and OM10.1 (HIV infected) cells were used as a myelocytic model, and Jurkat (parent) and J1.1 (HIV infected) cells were used as the lymphocytic model. All cell lines were infected with MG1 at MOI 10^{-5} to MOI 1 for 24 hours, after which cell death was measured using PI (**Figures 4B, 5B**) staining and level of infection was determined by eGFP expression using flow cytometry (**Figures 4A, 5A**).

3.1.1 Myelocytic cells

As anticipated, HIV infected OM10.1 cells were far more permissive to MG1 infection and killing than the healthy HL60 cells (**Figure 4A and B**), clearly demonstrating the ability of MG1 to selectively target HIV infected cells. eGFP expression increased in a dose-dependent manner starting at MOI 10^{-2} and then peaked at ~80% at MOI 10^{-1} and MOI 1 indicating high levels of infection at these MOI (**Figure 4A**). Cell death of OM10.1 cells followed a dose-

dependent response, peaking at ~ 80% of cells being PI+ at MOI 1. Both eGFP and cell death results reflecting previous work in our lab[148].The parental uninfected myelocytic cell line HL60 was not permissive to MG1 infection, with no cells eGFP+ at 24 h.p.i (**Figure 4A**). Cell death of HL60 cells remained comparable to the uninfected, at ~10% background cell death occurring at each MOI (**Figure 4B**). This is consistent with the likelihood that since HL60's are not HIV infected, they possess intact IFN signalling, thus making them refractory to MG1 killing.

3.1.2 Lymphocytic cells

Both Jurkat and J1.1 cells were highly permissible to infection with MG1 starting at MOI 10^{-4} with ~80% eGFP+ cells and eGFP levels remaining consistently high in both cell lines until MOI 1 (**Figure 5A**). Cell death was high beginning at MOI 10^{-4} for both cell lines with ~60% of cells PI+ and increasing steadily until MOI 1 (**Figure 5B**).

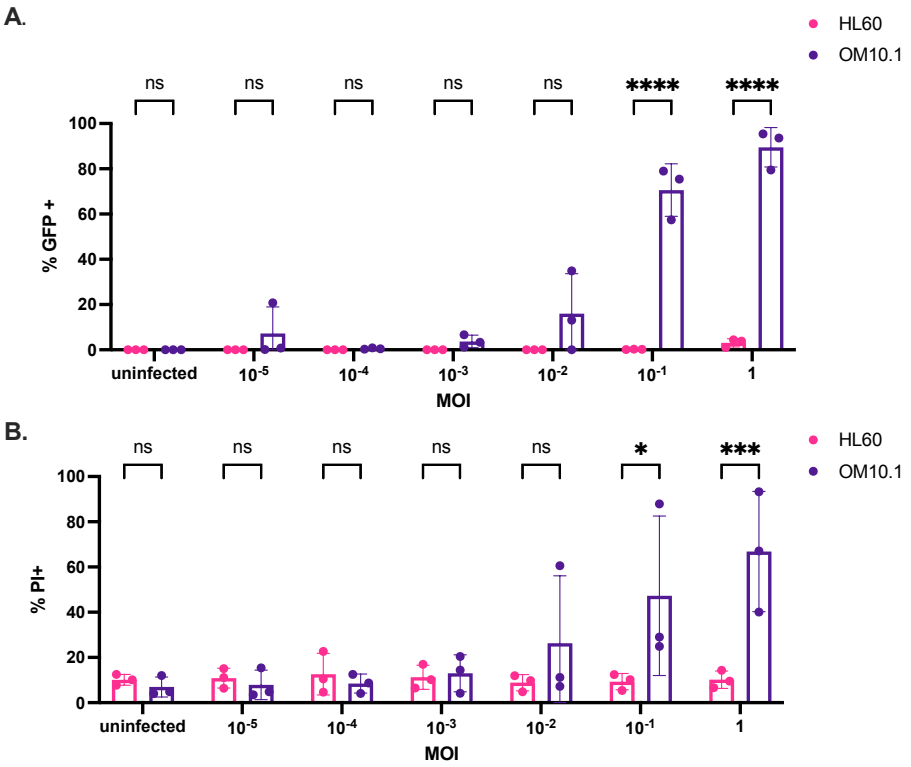
A.
HL60
OM10.1
ns
ns
ns
ns
ns
****
****
100
80
60
40
20
0
% GFP +
uninfected
10-5
10-4
10-3
10-2
10-1
1
MOI
B.
HL60
OM10.1
ns
ns
ns
ns
ns
*
***
100
80
60
40
20
0
% PI+
uninfected
10-5
10-4
10-3
10-2
10-1
1
MOI

Figure 4. HIV infected OM10.1 cells are preferentially infected and killed by MG1 over their uninfected parental cell line. Both OM10.1 and Hl60 cells were infected with MG1 at MOI 10^{-5} to MOI 1 or left uninfected for 24 hours in a 12 well plate. At 24 h.p.i, cells were stained with Propidium Iodide (PI) and analyzed on flow cytometry. eGFP+ cells (**A**) represent live cells infected with virus, while PI+ cells (**B**) represent dead cells. Two-way ANOVA with multiple comparisons test performed. ns = not significant, * = p-value < 0.05, *** = p-value < 0.001, **** = p-value < 0.0001. Data representing mean +/- SE (n = 3).

A.

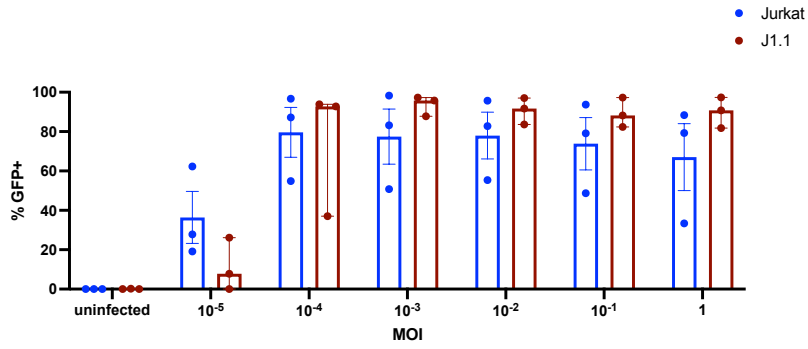
Jurkat
J1.1
% GFP+
100
80
60
40
20
0
uninfected
10-5
10-4
10-3
10-2
10-1
1
MOI

B.

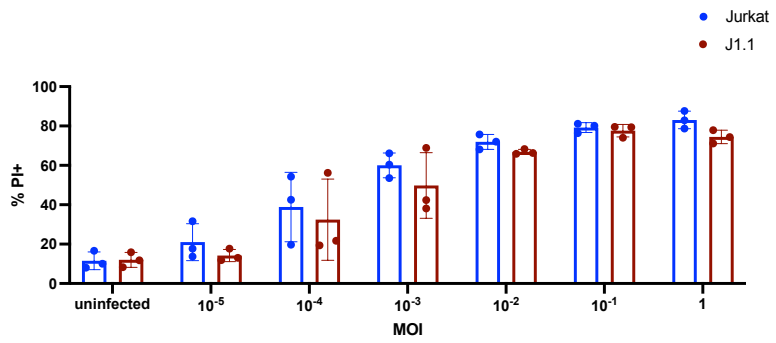
Jurkat
J1.1
% PI+
100
80
60
40
20
0
uninfected
10-5
10-4
10-3
10-2
10-1
1
MOI

Figure 5. Both Jurkat and J1.1 cell lines are permissible to infection with MG1 and cell death. Cells were infected with MG1 at MOI 10^{-5} to MOI 1 or left uninfected for 24 hours in a 12 well plate. At 24 h.p.i, cells were stained with Propidium Iodide (PI) and analyzed on flow cytometry. eGFP+ cells (**A**) represent live cells infected with virus, while PI+ cells (**B**) represent dead cells. Two-way ANOVA with multiple comparisons test performed. Data representing mean +/- standard error (SE), (n = 3).

3.2 MG1 induced cell death of HIV infected and uninfected cell lines

The following experiments were conducted to evaluate programmed cell death (PCD) processes in MG1 infected, HIV infected and uninfected cell lines. Furthermore, we also sought to determine if cell death mechanisms differ between HIV infected and uninfected cells. As HL60 cells were not permissible to MG1 infection, the Jurkat/J1.1 cell line pair was used as the primary model. OM10.1 cells were also evaluated on their own.

3.2.1 Uninfected (healthy) cells

Uninfected Jurkat cells were pre - treated with caspase inhibitors and infected with MG1 to evaluate whether caspases are involved in MG1-induced cell death of this cell line. The gating strategy for data analysis is shown in **supplementary figure 1**, and caspase inhibitors were optimized on all cell lines prior to experiments (**Supplementary figures 6, 7, and 8**).

Cells that were not MG1 infected but treated with the chemical inducer of apoptosis Staurosporine (STS), resulted in ~ 80% cell death as defined by % AnnexinV/PI+ (**Figures 6A and C**). In the presence of 50uM of either caspase inhibitor Z-VAD-FMK (**Figure 6A**) or Z-DEVD-FMK (**Figure 6C**), STS induced cell death was significantly decreased, confirming that these inhibitors are capable of partially abrogating cell death in this cell line.

In Jurkat cells treated with either Z-VAD-FMK or Z-DEVD-FMK and infected with MG1 at MOI 10^{-4} and MOI 10^{-2}, cell death decreased in comparison to cells infected with virus alone , indicating that MG1 induces caspase dependent cell death in Jurkat cells (**Figure 6**). From this, we conclude that caspases are involved in MG1 induced killing of Jurkat cells.

3.2.2 HIV infected cells

In HIV infected J1.1 cells, very minimal cell death was observed when cells were infected with MG1 at MOI 10^{-4}, and subsequently no changes in cell death could be detected in the presence of either Z-VAD-FMK (**Figure 7A**) or Z-DEVD-FMK (**Figure 7C**). At MOI 10^{-2}, cell death with virus alone was ~ 60% - however in the presence of caspase inhibitors cell death did not decrease as it did in Jurkat cells. Treatment with the pan-caspase inhibitor Z-VAD-FMK resulted in no change in cell death (**Figure 7A**), and treatment with the caspase 3 inhibitor Z-DEVD-FMK resulted in very minimal decreases in cell death (**Figure 7C**) however this did not reach statistical significance. When analyzed as relative change to control, J1.1 cells infected with MG1 at MOI 10^{-2} and treated with both caspase inhibitors showed no significant decreases in cell death (**Figures 7B and D**), thus leading to the conclusion that caspases are not involved in MG1-mediated killing of J1.1 cells.

Myelocytic OM10.1 cells, the HIV infected daughter cell line of HL60, treated with the chemical apoptosis inducer Camptothecin, underwent ~ 50-60% cell death, which decreased in the presence of Z-VAD-FMK (**Figure 8A**) and Z-DEVD-FMK (**Figure 8C**), confirming that the inhibitors can abrogate caspase activity and reduce cell death in this cell line. When MG1 MOI 10^{-2} was used to induce cell death, the presence of either Z-VAD-FMK (**Figure 8A**) or Z-DEVD-FMK (**Figure 8C**) had no significant impact on the proportion of cells that were AnnexinV/PI+. Relative to the control, changes in cell death were not statistically significant in the presence of either inhibitor (**Figures 8B and D**). These findings are consistent with results from the J1.1 cell line, whereby caspases are not involved in MG1 induced cell death of myelocytic OM10.1 cells,

further suggesting that caspases are not involved in MG1 mediated cell death of HIV infected cell lines.

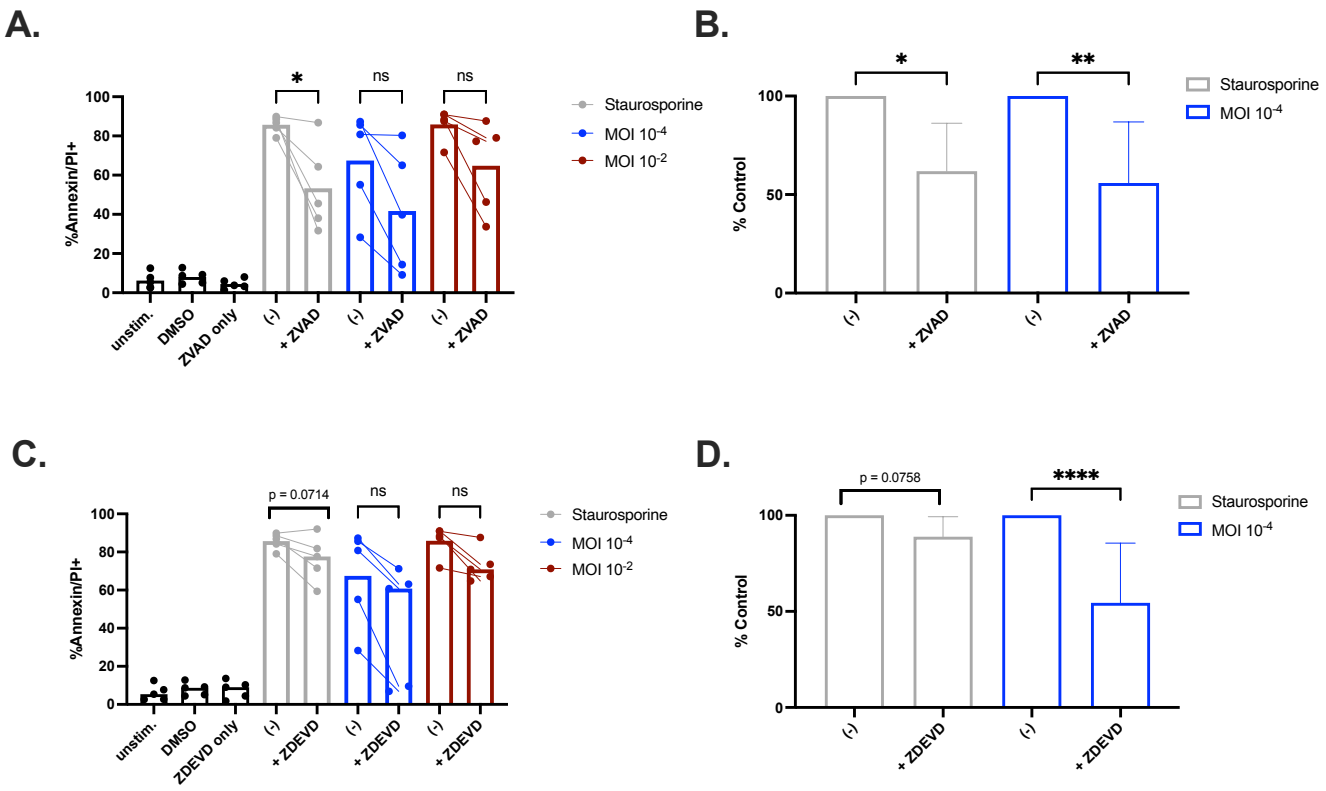
A.
%Annexin/PI+
100
80
60
40
20
0
*
ns
ns
unstim.
DMSO
ZVAD only
(-)
+ ZVAD
(-)
+ ZVAD
(-)
+ ZVAD
Staurosporine
MOI 10-4
MOI 10-2
B.
% Control
100
50
0
*
**
(-)
+ ZVAD
(-)
+ ZVAD
Staurosporine
MOI 10-4
C.
%Annexin/PI+
100
80
60
40
20
0
p = 0.0714
ns
ns
unstim.
DMSO
ZDEVD only
(-)
+ ZDEVD
(-)
+ ZDEVD
(-)
+ ZDEVD
Staurosporine
MOI 10-4
MOI 10-2
D.
% Control
100
50
0
p = 0.0758
****
(-)
+ ZDEVD
(-)
+ ZDEVD
Staurosporine
MOI 10-4

Figure 6. Jurkat cells undergo caspase-dependent cell death during MG1 infection. Jurkat cells were pre-treated for 1 hour with 50uM of Z-VAD-FMK (**A**) or Z-DEVD-FMK (**C**), after which they were infected with MG1 at MOI 10^{-4}, 10^{-2}, or left uninfected. As a positive control, some cells were treated with 2uM of the chemical apoptosis inducer Staurosporine. At 24 h.p.i, cells were stained with AnnexinV/PI stain and cell death was analyzed using flow cytometry. Data also shown relative to the control (**B, D**). Student's T test analysis performed whereby ns = not significant, * = p-value < 0.05, ** = p-value < 0.01, and **** = p-value < 0.0001 (n = 5).

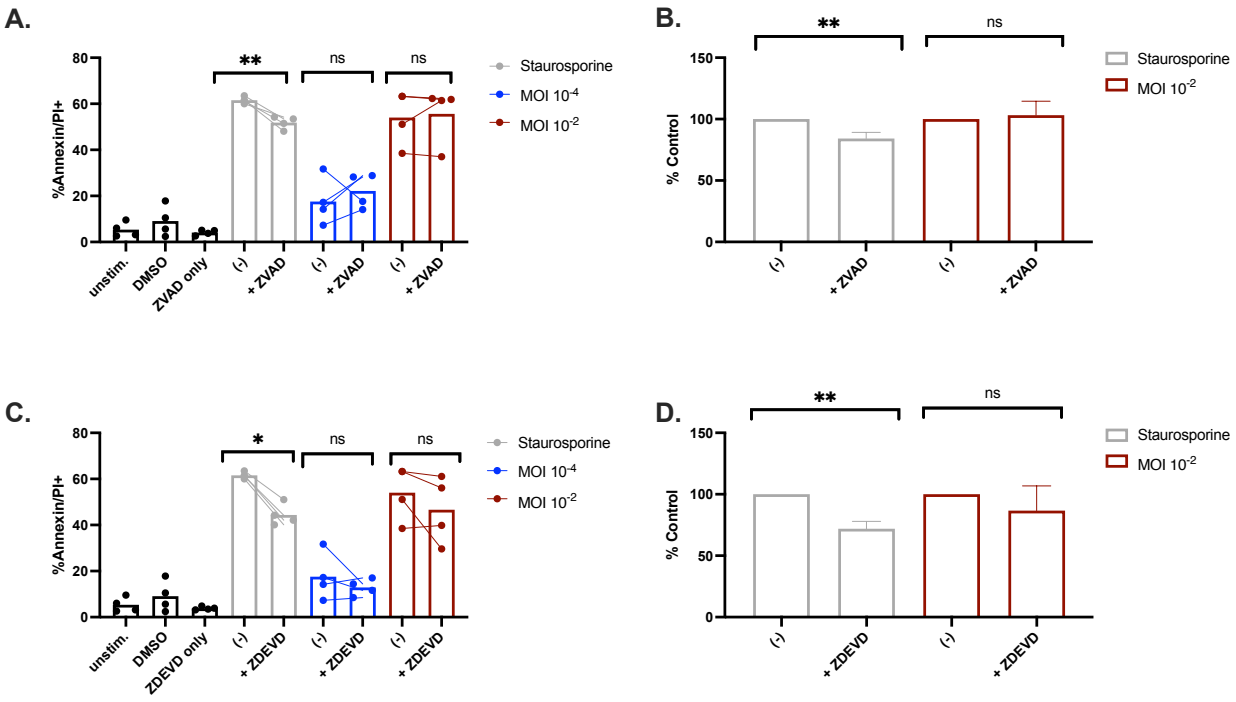
A.
%Annexin/PI+
80
60
40
20
0
**
ns
ns
unstim.
DMSO
ZVAD only
(-)
+ ZVAD
(-)
+ ZVAD
(-)
+ ZVAD
Staurosporine
MOI 10-4
MOI 10-2
B.
% Control
150
100
50
0
**
ns
(-)
+ ZVAD
(-)
+ ZVAD
Staurosporine
MOI 10-2
C.
%Annexin/PI+
80
60
40
20
0
*
ns
ns
unstim.
DMSO
ZDEVD only
(-)
+ ZDEVD
(-)
+ ZDEVD
(-)
+ ZDEVD
Staurosporine
MOI 10-4
MOI 10-2
D.
% Control
150
100
50
0
**
ns
(-)
+ ZDEVD
(-)
+ ZDEVD
Staurosporine
MOI 10-2

Figure 7. Caspases are not involved in MG1-induced cell death of HIV infected J1.1 cells. J1.1 cells were pre-treated for 1 hour with 50uM of Z-VAD-FMK (**A**) or Z-DEVD-FMK (**C**), after which they were infected with MG1 at MOI 10^{-4}, 10^{-2}, or left uninfected. As a positive control, some cells were treated with 10uM of the chemical apoptosis inducer Staurosporine. At 24 h.p.i, cells were stained with AnnexinV/PI stain and cell death was analyzed using flow cytometry. Data also shown relative to the control (**B, D**). Student's T test analysis performed whereby ns = not significant, * = p-value < 0.05, and ** = p-value < 0.01 (n = 4).

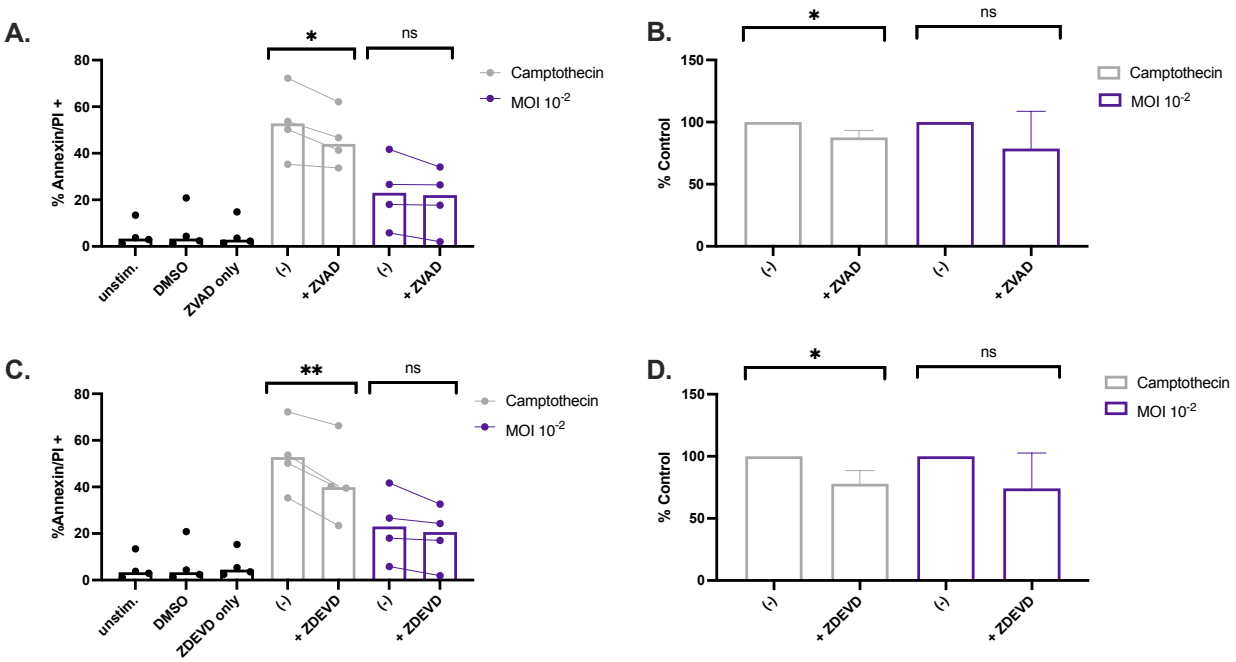
A.
*
ns
% Annexin/PI +
80
60
40
20
0
unstim.
DMSO
ZVAD only
(-)
+ ZVAD
(-)
+ ZVAD
Camptothecin
MOI 10-2
B.
*
ns
% Control
150
100
50
0
(-)
+ ZVAD
(-)
+ ZVAD
Camptothecin
MOI 10-2
C.
**
ns
%Annexin/PI +
80
60
40
20
0
unstim.
DMSO
ZDEVD only
(-)
+ ZDEVD
(-)
+ ZDEVD
Camptothecin
MOI 10-2
D.
*
ns
% Control
150
100
50
0
(-)
+ ZDEVD
(-)
+ ZDEVD
Camptothecin
MOI 10-2

Figure 8. Caspases are not involved in MG1-induced cell death of HIV infected OM10.1 cells. OM10.1 cells were pre-treated for 1 hour with 50uM of Z-VAD-FMK (**A**) or Z-DEVD-FMK (**C**), after which they were infected with MG1 at MOI 10^{-2} or left uninfected. As a positive control, some cells were treated with 0.2uM of the chemical apoptosis inducer Camptothecin. At 24 h.p.i, cells were stained with AnnexinV/PI stain and cell death was analyzed using flow cytometry. Data also shown relative to the control (**B, D**). Student's T test analysis performed whereby ns = not significant, * = p-value < 0.05, and ** = p-value < 0.01 (n = 4).

3.3 HIV infected cell lines have decreased caspase 3 and 7 expression

Given the results presented in section 3.2, it appears that MG1 induces caspase-dependent cell death in Jurkat cells, however caspases are not involved in MG1- mediated cell death of the HIV infected cell lines, concluding that PCD mechanisms are different in HIV infected cells. We thus sought to investigate caspase 3 and 7 activity during MG1 infection in Jurkat vs J1.1's, and OM10.1 cells to see if caspase levels could further explain our findings.

All cell lines were infected with MG1 at MOI 10^{-2} for 24 hrs, after which caspase 3/7 activity was measured using the FLICA 660 stain for flow cytometry. It is first important to note that uninfected cells did not demonstrate any caspase activity. When Jurkat and J1.1 cells were infected with MG1, we observed a significant difference in caspase activity in Jurkat cells compared to their HIV infected counterpart – J1.1 cells. 90-95% of Jurkat cells had active caspase 3/7, whereas J1.1 cells had approximately 30% of cells caspase 3/7 + (**Figure 9B**). 80% of eGFP+ Jurkat cells (i.e MG1 infected) had caspase 3/7 activity and only ~ 3% of J1.1 did so, indicating a highly significant difference between the two cell lines (**Figure 9D**).

In OM10.1 cells, we again observe no caspase activity in the unstimulated condition. When these cells were infected with MG1, very low levels of caspase activity was observed, with ~ 5% of the population expressing caspase 3/7 (**Figure 10B**) and approximately the same levels seen when gated on the eGFP+ (MG1 infected) population (**Figure 10D**). Given that both HIV infected cell lines express such little caspase activity during infection with MG1, it is not surprising that the results in section 3.2 indicate caspase-independent cell death occurring during MG1 infection, adding to our conclusion that MG1 induced cell death is different

between HIV infected and uninfected cells, and offer a possible explanation as to why these cell lines appear to undergo PCD independent of caspases.

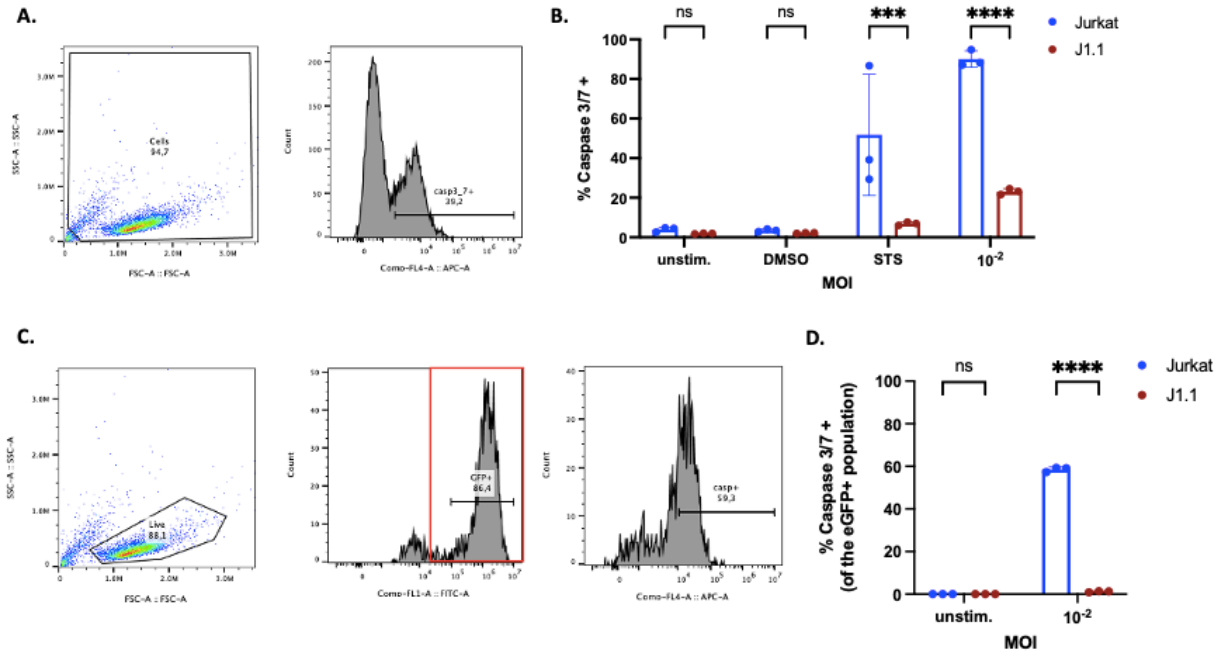
A.
Cells
94,7
SSC-A :: SSC-A
FSC-A :: FSC-A
Count
casp3_7+
39,2
Comp-FL4-A :: APC-A
B.
ns
ns
***
****
Jurkat
J1.1
% Caspase 3/7 +
100
80
60
40
20
0
unstim.
DMSO
STS
10-2
MOI
C.
Live
88,1
SSC-A :: SSC-A
FSC-A :: FSC-A
Count
GFP+
86,4
Comp-FL1-A :: FITC-A
Count
casp+
59,3
Comp-FL4-A :: APC-A
D.
ns
****
Jurkat
J1.1
% Caspase 3/7 +
(of the eGFP+ population)
100
80
60
40
20
0
unstim.
10-2
MOI

Figure 9. J1.1 cells have lower caspase 3/7 expression compared to the healthy Jurkat cells during MG1 infection. Jurkat and J1.1 cells were plated and infected with MG1 at MOI 10^{-2}, left uninfected, or treated with 2uM (Jurkat) or 10uM (J1.1) of Staurosporine (STS). At 24 h.p.i, cells were collected for flow cytometry. Cells were stained using the FLICA 660 caspase 3/7 staining kit. Gating strategy for measuring bulk caspase 3/7 expression in all cells (**A**), caspase expression in bulk cell population (**B**), gating strategy for measuring caspase expression in the eGFP+ cell population (**C**), and caspase expression of the MG1 infected eGFP+ population (**D**). Two-way ANOVA with multiple comparisons performed whereby ns = not significant, *** = p-value < 0.001, **** = p-value < 0.0001. Data shown as mean +/- SE (n = 3).

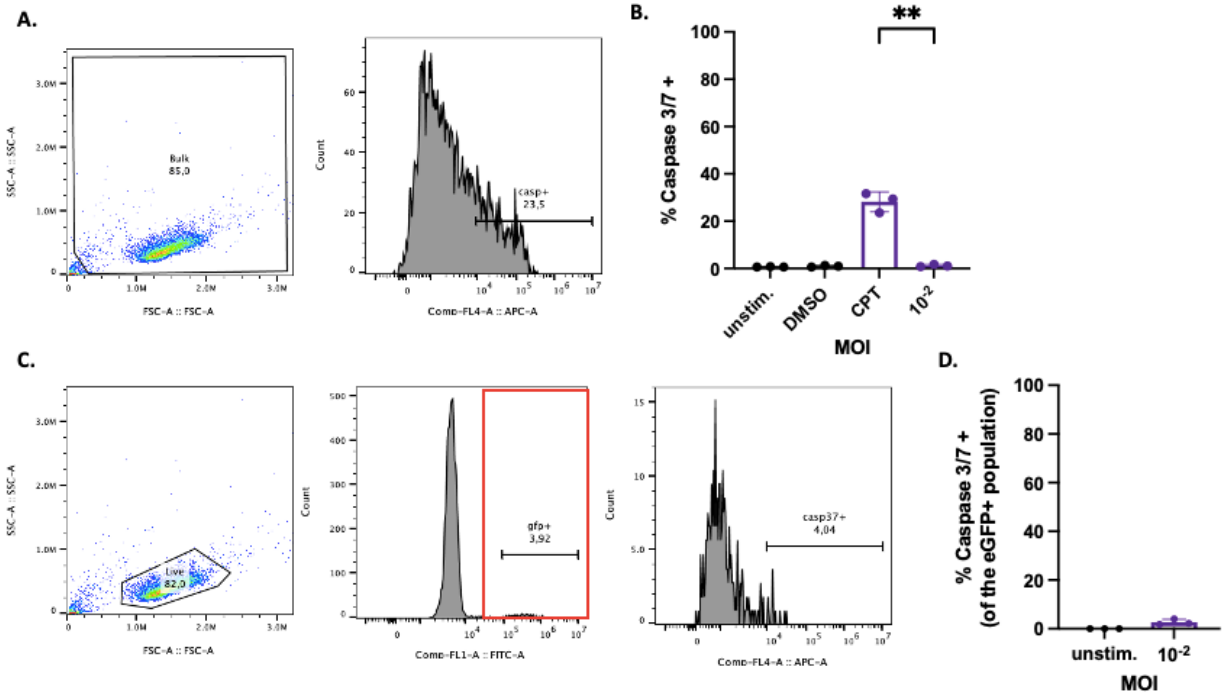
A.
Bulk
85,0
FSC-A :: FSC-A
SSC-A :: SSC-A
casp+
23,5
Count
Comp-FL4-A :: APC-A
B.
**
% Caspase 3/7 +
unstim.
DMSO
CPT
10-2
MOI
C.
Live
82,0
gfp+
3,92
casp37+
4,04
Comp-FL1-A :: FITC-A
D.
% Caspase 3/7 +
(of the eGFP+ population)
unstim.
10-2
MOI

Figure 10. HIV infected OM10.1 cells have decreased caspase 3/7 expression during MG1 infection. OM10.1 cells were plated and infected with MG1 at MOI 10^{-2}, left uninfected, or treated with 0.2uM Camptothecin (CPT). At 24 h.p.i, cells were collected for flow cytometry. Cells were stained using the FLICA 660 caspase 3/7 staining kit. Gating strategy for measuring bulk caspase 3/7 expression in all cells (**A**), caspase expression in bulk cell population (**B**), gating strategy for measuring caspase expression in the eGFP+ cell population (**C**), and caspase expression of the MG1 infected eGFP+ population (**D**). Paired student's T test performed whereby ** = p-value > 0.01. Data shown as mean +/- SE (n = 3).

3.4 HIV infected MDM are preferentially killed by MG1

Next, we sought to examine MG1 induced killing in a primary cell model. We used monocyte-derived macrophages (MDM) isolated from PBMC via plate adherence and infected them with an R5 tropic HSA expressing virus HIV BAL IRES HSA. This strain of HIV gains entry into the cell using the CCR5 co-receptor and infected cells express the murine heat stable antigen (HSA) on their cell surface. Since the true pool of cells infected with HIV *in vitro* is quite small, using this strain allows us the classify cells as HSA+ being HIV infected and HSA- being HIV uninfected – thus we can exclude the bystander cells and analyze only those truly infected with HIV.

At 7 days post monocyte isolation, macrophages were infected with 100ng of HIV for 6 days or an equivalent volume of PBS was added to the uninfected control. At 6 d.p.i, cells were infected with MG1 for 24 hours at MOI 1, 5, 10 or left uninfected. Cells were stained with anti-HSA and AnnexinV and flow cytometry was performed. The gating strategy is depicted in **Figure 11A**.

When MDM were infected with MG1, both HSA+ and HSA- populations were permissive to MG1 infection, with eGFP levels ranging from 20-30% for both populations. A dose-dependent increase in eGFP expression is also noted (**Figure 11B**). Although the HSA- population expressed higher levels of eGFP than the HSA+, these numbers are small and statistically not significant (**Figure 11B**).

Although both populations appear to be equally permissive to MG1 infection, the HSA+ population undergoes more cell death during infection with OV, as evident by higher levels of AnnexinV in the HSA+ population than the HSA-counterparts (**Figure 11C**), suggesting that HSA+

cells are preferentially killed by MG1 over the uninfected bystander cells – a finding that corroborates previous work by our group[149].

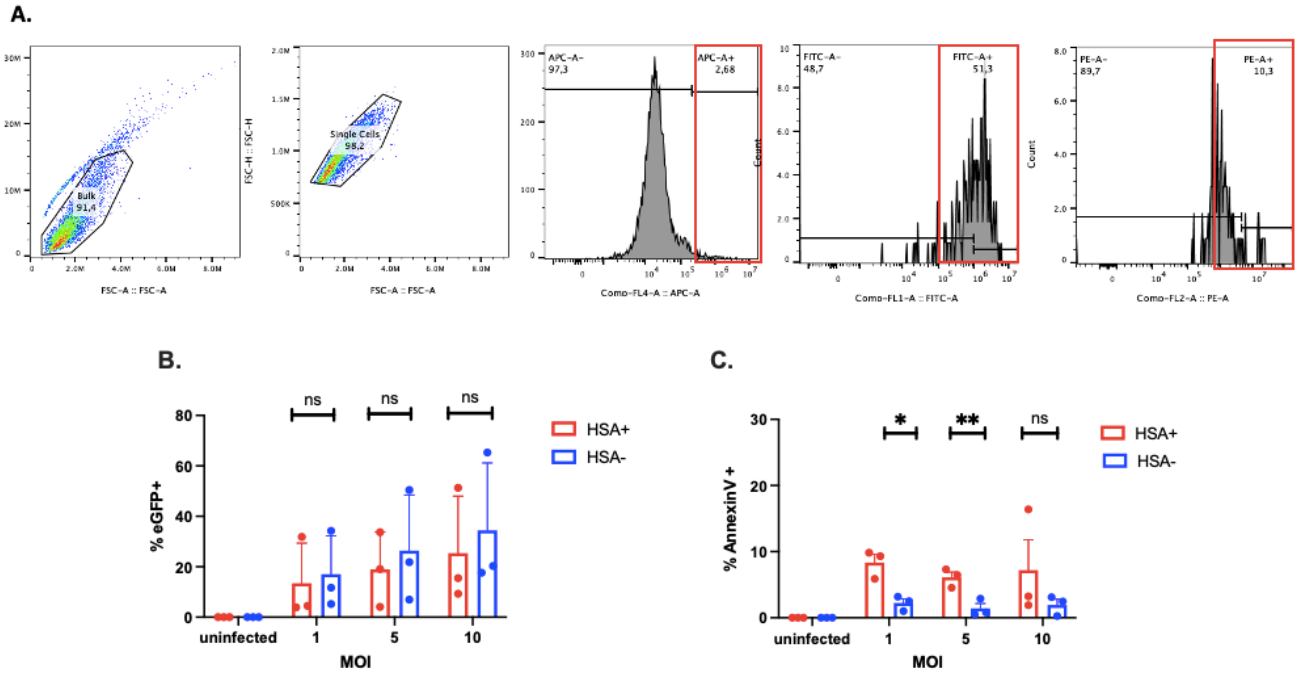
A.
Bulk
91,4
FSC-A :: FSC-A
FSC-H :: FSC-H
Single Cells
98,2
FSC-A :: FSC-A
APC-A-
97,3
APC-A+
2,68
Comp-FL4-A :: APC-A
FITC-A-
48,7
FITC-A+
51,3
Comp-FL1-A :: FITC-A
PE-A-
89,7
PE-A+
10,3
Comp-FL2-A :: PE-A
Count
B.
% eGFP+
ns
ns
ns
uninfected
1
5
10
MOI
HSA+
HSA-
C.
% AnnexinV+
*
**
ns
uninfected
1
5
10
MOI
HSA+
HSA-

Figure 11. Both HIV infected (HSA+) and uninfected (HSA-) populations are permissive to MG1 infection, and HIV infected cells are preferentially killed by MG1. Primary MDM were isolated from whole blood via plate adherence and infected with 100ng of HIV for 6 days or left uninfected. At 6 d.p.i, cells were infected with MG1 for 24 hours at MOI 1, 5, 10 or left uninfected. Cells were stained with AnnexinV and anti-HSA. HSA+ cells are considered HIV infected, and HSA- cells are HIV uninfected. eGFP (**B**) and AnnexinV (**C**) expression was analyzed using flow cytometry. Gating strategy depicted in (**A**). Paired student's T test performed between HSA+/HSA- populations. * = p-value < 0.05, ** = p-value < 0.01. Data shown as mean + SE (n = 3).

Chapter 4: Discussion

The results herein indicate that MG1 is capable of preferential infection and killing of HIV infected cell lines, with OM10.1's infected and killed to a much higher degree than their uninfected counterpart, and both Jurkat and J1.1's being highly permissive to MG1 infection and killing. Furthermore, HIV infected MDM are preferentially killed by MG1 over the uninfected bystander cells *in vitro*. When examining cell death during MG1 infection of cell lines, caspase inhibitors were used to determine if MG1-induced cell death is caspase-dependent. The results indicate that MG1 induces a caspase-dependent cell death pathway in Jurkat cells, however caspases do not seem to be involved in cell death of HIV infected cells, concluding that PCD mechanisms differ in the presence of HIV. We next investigated caspase 3 and 7 expression levels in cell lines during MG1 infection. Interestingly, HIV infected J1.1 and OM10.1 cells had lower levels of caspase 3 and 7 than the uninfected Jurkat cells, suggesting a possible explanation as to why MG1 does not induce caspase-dependent cell death in these cell lines. Further investigation into different types of cell death in both HIV infected cell lines and primary cells is required in order to fully elucidate the mechanism of MG1-mediated killing.

4.1 MG1 preferentially infects HIV infected cell lines, and preferentially kills both HIV infected cell lines and primary MDM

4.1.1 Cell Lines

As mentioned previously, it is known that MG1 targets and kills cells with defects in the antiviral IFN signalling cascade. Thus, it is expected that MG1 will preferentially infect and kill HIV infected cells over their uninfected counterparts due to IFN signalling impairments in HIV infected cells. In this work, MG1 preferentially infected both HIV- infected OM10.1 cells and J1.1 cells (**Figures 4 and 5**), a result that has been previously demonstrated in our lab ([148] and Ranganath, N*. unpublished*). Jurkat cells were also highly permissive to MG1 infection and killing (**Figure 5**). Since Jurkat cells are an immortalised cancer cell line, it is highly likely they possess IFN signalling impairments, rendering them permissive to MG1 infection. For example, reduced expression of interferon - γ receptor 2 (IFN-γR2) has been identified in Jurkat cells[177].

It was also noted that HL60 cells were not permissible to MG1 infection. Previously, our lab investigated IFN signalling in HL60 cells and found that baseline levels of IFNAR1, ISG15, and MHC-1 are much higher than in OM10.1 cells, indicating that HL60 cells do not appear to possess IFN signalling impairments[178]. It is likely that HL60 cells were not permissible to MG1 infection due to the presence of intact IFN signalling, thus attenuating OV infection.

4.1.2 Primary MDM

In primary macrophages, our results indicate that although both HSA+ and HSA- cells are infected with MG1 to a similar degree, HIV infected cells (HSA+) are preferentially killed by MG1 over the uninfected bystander cells (**Figure 11C**), demonstrating the ability of MG1 to target HIV infected primary cells *in vitro* while sparing the bystanders – a result that has also been replicated in previous work from our group[149].

HIV infected macrophages have been found to possess IFN signalling impairments, making them a target for MG1 induced cell death and elimination. Our group has demonstrated downregulation of two interferon stimulated genes (ISG's), PKR and ISG15 in HIV infected MDM (HSA+) when compared to HSA- cells[149]. Furthermore, Harman and colleagues demonstrated that HIV infected macrophages fail to express type I and type III ISG's *in vitro*, and that HIV accessory proteins Vpr and Vif bind to and inhibit TANK binding kinase 1 (TBK1), thus perturbating the release of IFN[179]. Others have also reported downregulation of IFN-α/β receptor *in vivo*[180], and impaired STAT1/2 activation via HIV Tat[181].

Our group has also demonstrated the ability of MG1 to eliminate HIV infected macrophages *ex vivo* using alveolar macrophages (AM) from cART treated PLWHIV[149]. Both *in vitro* findings such as those presented herein and *ex vivo* findings are necessary towards developing MG1 for clinical use as an HIV cure.

4.2 MG1 – induced cell death of cell lines differs between HIV infected and uninfected cells

Our results indicate that cell death of MG1 infected Jurkat cells decreases upon pre-incubation with caspase inhibitors (**Figure 6**). However, the same result was not seen in the HIV infected J1.1 or OM10.1 cells (**Figures 7 and 8**), suggesting that cell death during MG1 infection is different in the presence of HIV infection.

Viruses can induce different cell death pathways upon changes in protein expression. The most common example is virus induced inhibition of caspase-8. When caspase-8 is inhibited, it no longer supresses RIPK1/3, thus leading to the activation of RIPK1/3 and initiation of necroptosis. Viruses such as cytomegalovirus (CMV), bovine herpesvirus-4 (BHV-4),

adenovirus, and HSV- 1/2 have all been shown to inhibit caspase-8 activity, thus preventing apoptosis (reviewed in [182]). It is possible that HIV viral proteins interfere with cell death proteins, thus forcing the HIV infected cells to undergo cell death through caspase-independent mechanisms. Since treatment with caspase inhibitors did not reduce cell death in HIV infected J1.1 or OM10.1 cells during MG1 infection, it is presumed that caspase-independent mechanisms of cell death occur.

Viruses can also induce different means of cell death in different cell types. For example, Influenza A virus (IAV) is known to induce apoptosis, necroptosis, and pyroptosis[183–187]. IAV has been shown to induce apoptosis in airway epithelial cells[183], macrophages[188], and monocytes[189], whereas it can induce necroptosis in dendritic cells (DC's)[185]. SARS-CoV-2 virus has recently been shown to induce apoptosis of pulmonary epithelial cells in human and non-human primate (NHP) lungs as well as induce pyroptosis in haematopoietic stem cells[190,191] VSV – an oncolytic virus in the same family as MG1 has been shown to induce both apoptosis and necroptosis in esophageal cancer cells[192], as well as induce NL3P3 inflammasome activation (a characteristic of pyroptosis) in murine bone marrow derived macrophages (BMDM)[193]. Given the many genetic and structural similarities between VSV and MG1, it is likely that MG1 can also induce multiple cell death pathways.

Our results closely resemble those of Bolton et al. where the caspase inhibitors Z-VAD-FMK and BocD-FMK failed to abolish cell death of HIV NL4.3 HSA infected Jurkat cells, leading the authors to conclude that cell death of HIV infected CD4+ T cell lines is independent of caspases or apoptosis[194]. Given the similarities between these results and ours, we speculated that the same is occurring during MG1 infection and perhaps caspase activity in our HIV

infected cell lines may be different than healthy cells. This hypothesis drove us to investigate caspase 3 and 7 activity levels in cell lines during MG1 infection.

4.3 MG1 induced cell death of HIV infected cell lines is independent of caspase activity

We have demonstrated that in HIV infected cell lines, caspase activity during infection with MG1 is significantly lower than that observed in HIV-uninfected cells, possibly explaining why HIV infected cell lines appear to undergo caspase independent cell death during MG1 infection. Consistent with this, the 2002 study by Bolton and colleagues demonstrated decreased caspase activity in HIV infected H9T cells when treated with Staurosporine when compared to uninfected staturosporine treated H9 T cells[194]. It is also known that several viruses have evolved mechanisms to block cellular apoptosis to keep the cell alive, hence supporting viral survival (reviewed in [195]).

Viral proteins can interact with caspases - for example, CrmA is a protein encoded by poxviruses and is one of the most studied viral caspase inhibitors, abrogating apoptosis by inhibition of caspase-8 or sometimes caspase-1[196]. The baculovirus encoded protein p35 can inhibit mammalian caspases 1, 3, 6, 7, 8, and 10[197] and has been shown to render murine thymocytes resistant to apoptosis – inducing agents[198]. Furthermore, Herpes-simplex virus 1 (HSV - 1) has been shown to block caspase-3 and caspase-dependent cell death in infected cell lines[199], murine cytomegalovirus (MCMV) M36 protein has been shown to inhibit caspase-8 activation in murine cell lines[200], and Vaccinia virus B13R protein is known to target caspases[201]. HIV interference with caspase activity could explain the decreased caspase activity recorded here (**Figures 9 and 10**).

Like other viral infections, caspase activity can be downregulated in HIV infection. For example, Cai. and colleagues determined that caspase-1 activity is downregulated in CD4+ T cells from PLWHIV and undergoing cART[202]. Furthermore, Pan. and colleagues demonstrated cell death via necroptosis in HIV infected primary CD4+ T cells and HIV infected Jurkat cells[203]. In 2021, Terahara. and colleagues found that necroptosis is induced in HIV infected CD4+ T cells in a humanized mouse model[204]. Since necroptosis most commonly requires caspase-8 inhibition to proceed, one can hypothesize that caspase-8 is downregulated in this model, however the authors of the above studies did not report this. In a 2008 study by Fernandez Larrosa. and colleagues, caspase 3 activity in HIV infected J1.1 cells very closely resembled our results in that caspase activity in Jurkat cells was 3-fold higher than J1.1 cells (**Figure 9**). The authors of the above study reported ~ 1% of J1.1 cells with active caspase-3 upon cell death induced with Staurosporine – compared to 30% of Jurkat cells having active caspase-3[205].

We reported decreased caspase 3 and 7 expression in HIV infected cell lines, a result similar to Tanaka. and colleagues[206]. The authors found decreased caspase 3 expression in TNF-α and Camptothecin treated HIV infected 26L cells (a subclone of pro – monocytic U937 cell line). Furthermore, the cells appeared to undergo caspase-3 independent cell death[206]. This further corroborates our findings that HIV infection interferes with caspases, thus making cells resistant to caspase-dependent cell death.

To conclude, MG1 induced cell death differs between HIV-infected and uninfected cells. HIV infected cell lines undergo caspase-independent cell death during viral infection with MG1, whereas Jurkat cells undergo caspase-dependent cell death. Furthermore, caspase 3 and 7

activity is downregulated in HIV infected cell lines, a factor likely contributing to the observed caspase-independent cell death.

4.4 Limitations and Future Directions

One of the primary limitations of this study is the use of immortalised cell lines. As briefly mentioned, cancer cell lines contain genetic mutations which may impact cellular processes. For example, mutations in the CTLA-4 and SYK genes have been identified in Jurkat cells, causing irregularities in TCR signalling[207] and conferring resistance to apoptosis[208]. The precise differences between cell death mechanisms in our cell lines versus primary cells are unclear, however using a primary cell model of CD4+ T lymphocytes and expanding on our monocyte-derived macrophage work would certainly be a necessary future step for this work.

The use of chemical caspase inhibitors is a limitation of this study. Although our inhibitors did successfully abrogate caspase activity to a certain extent, they did not fully block caspases (**Supplementary figures 6C and D, 7C and D, and 8C and D**). To achieve full inhibition of caspase activity, genetic knockout studies would be necessary and would likely add additional confidence to the results.

Another caveat of the cell line work is that MG1 is an oncolytic virus, thus it can effectively infect and kill cancer cells. Given this, MG1 can infect and kill even our "healthy" Jurkat cells. To truly distinguish the ability of MG1 to target HIV infected cells over the bystanders, using our HSA sorted MDM model is necessary. Future experiments will include examining MG1 induced cell death using caspase inhibitors on MDM, something that has been

briefly examined in our lab. Previously, we have measured apoptosis in HIV infected MDM in the presence of Z-VAD-FMK and a chemical inhibitor of necroptosis,Necrostatin-1. These results, albeit preliminary, show no differences in cell death between HIV infected MDM treated with chemical cell death inhibitors as compared to untreated cells. Future work will include expanding on these experiments by using additional inhibitors such as Caspase-1 and Caspase-3 specific inhibitors (ex: Z-DEVD-FMK)[209]. This method will allow us to distinguish between the HIV infected and uninfected populations and provide needed insight towards MG1 induced PCD mechanisms in HIV infected primary cells.

Another primary cell model that would expand on this work is the use of a T cell model, which has been used in our lab previously[148]. Primary CD4+ T cells are isolated from PBMC, after which cells can be infected with MG1, and cell death can be analyzed. Similar to the use of MDM, this model serves more physiological relevance.

To further expand on the results of this work, future experiments should be performed to examine different cell death pathways in more detail. For example, we concluded that HIV infected cells undergo caspase-independent cell death during MG1 infection, however the question that remains is – what type of cell death is this? Further experiments examining necroptosis using RIPK1/2 inhibitors or autophagy would be necessary to reach a more precise conclusion. Furthermore, although we did conclude that Jurkat cells undergo caspase-dependent cell death, it would be interesting to determine the exact mechanism(s) thereof. Caspase-dependent cell death could be apoptotic, or pyroptotic – each with different outcomes on a physiological scale (ex: pro vs. anti-inflammatory). Further experiments into the role of caspases would be necessary.

4.5 Summary and Significance

To summarize, our findings indicate that MG1 can selectively target and kill HIV infected cell lines over the healthy parent cell lines, and preferentially kill HIV infected primary MDM over the bystander cells. We also conclude that MG1 induced cell death differs between HIV infected and uninfected cells, with HIV uninfected cells undergoing caspase-dependent cell death, and HIV infected cells undergoing caspase-independent cell death. Furthermore, caspase activity is significantly decreased in HIV infected cell lines, thus identifying that the mechanism of PCD is caspase independent.

This work has many implications towards an HIV cure. The use of MG1 as an oncolytic virotherapy is currently undergoing clinical trials for the treatment of various cancers (NCT02285816). We wish to follow suit and develop MG1 for use as a potential HIV cure and have just begun work testing the safety of MG1 on humanised mice (Aloufi, N. *not yet published*). Determining the mechanism of cell death induced by MG1 is of key importance required to push this development further as different cell death pathways induce various physiological responses *in vivo* (ex: inflammation, cytokine release, etc). For example, pyroptosis is pro-inflammatory and involves the release of danger associated molecular patterns (DAMP's) and cytokines[159] which could result in immune activation, whereas apoptosis is anti-inflammatory - both PCD pathways having different outcomes *in vivo*. With the examination of programmed cell death pathways, we hope to gain insight towards how MG1 can eradicate the latent and persistent HIV reservoirs, and hopefully become one step closer to a cure for HIV.

References

1. Gao, F. *et al.* Origin of HIV-1 in the chimpanzee Pan troglodytes troglodytes. *Nature* **397**, 436–441 (1999).
2. Faria, N. R. *et al.* HIV epidemiology. The early spread and epidemic ignition of HIV-1 in human populations. *Science* **346**, 56–61 (2014).
3. Durack, D. T. Opportunistic infections and Kaposi's sarcoma in homosexual men. *The New England journal of medicine* **305**, 1465–1467 (1981).
4. Gottlieb, M. S. Pneumocystis pneumonia--Los Angeles. 1981. *Am. J. Public Health* **96**, 980–983 (2006).
5. Update on acquired immune deficiency syndrome (AIDS)--United States. *MMWR. Morb. Mortal. Wkly. Rep.* **31**, 507-508,513-514 (1982).
6. Barré-Sinoussi, F. *et al.* Isolation of a T-lymphotropic retrovirus from a patient at risk for acquired immune deficiency syndrome (AIDS). *Science* **220**, 868–871 (1983).
7. Coffin, J. *et al.* What to call the AIDS virus? *Nature* **321**, 10 (1986).
8. Abdel-rahman, R. M., Makki, M. S. T. & Al-romaizan, A. N. Synthesis of Novel Fluorine Substituted Isolated and Fused Heterobicyclic Nitrogen 1 , 2 , 4-Triazin-5-One Moiety as Potential Inhibitor towards HIV-1 Activity. 247–268 (2014).
9. Lange, J. M. A. & Ananworanich, J. The discovery and development of antiretroviral agents. *Antivir. Ther.* **19 Suppl 3**, 5–14 (2014).
10. Health, G., Strategy, S. & Aids, T. E. *Hiv 2016–2021*. (2021).
11. United Nations Joint Programme on HIV/AIDS (UNAIDS). To help end the AIDS epidemic. *United Nations* 40 (2014).
12. Seitz, R. Human Immunodeficiency Virus (HIV). *Transfus. Med. Hemotherapy* **43**, 203–222 (2016).
13. Eisinger, R. W., Dieffenbach, C. W. & Fauci, A. S. HIV Viral Load and Transmissibility of HIV Infection: Undetectable Equals Untransmittable. *JAMA* **321**, 451–452 (2019).
14. John-Stewart, G. *et al.* Breast-feeding and Transmission of HIV-1. *J. Acquir. Immune Defic. Syndr.* **35**, 196–202 (2004).
15. Cunningham, A. L., Donaghy, H., Harman, A. N., Kim, M. & Turville, S. G. Manipulation of

dendritic cell function by viruses. *Curr. Opin. Microbiol.* **13**, 524–529 (2010).

16. Feng, Y., Broder, C. C., Kennedy, P. E. & Berger, E. A. HIV-1 entry cofactor: functional cDNA cloning of a seven-transmembrane, G protein-coupled receptor. *Science* **272**, 872–877 (1996).
17. Stein, B. S. *et al.* pH-independent HIV entry into CD4-positive T cells via virus envelope fusion to the plasma membrane. *Cell* **49**, 659–668 (1987).
18. Sousa, R., Chung, Y. J., Rose, J. P. & Wang, B.-C. Crystal structure of bacteriophage T7 RNA polymerase at 3.3 Å resolution. *Nature* **364**, 593–599 (1993).
19. Pan, X., Baldauf, H.-M., Keppler, O. T. & Fackler, O. T. Restrictions to HIV-1 replication in resting CD4+ T lymphocytes. *Cell Res.* **23**, 876–885 (2013).
20. Checkley, M. A., Luttge, B. G. & Freed, E. O. HIV-1 envelope glycoprotein biosynthesis, trafficking, and incorporation. *J. Mol. Biol.* **410**, 582–608 (2011).
21. Kuiken, C. *et al. HIV Sequence Compendium 2010*. (2010). doi:10.2172/1223877
22. Ananworanich, J. *et al.* Impact of multi-targeted antiretroviral treatment on gut T cell depletion and HIV reservoir seeding during acute HIV infection. *PLoS One* **7**, e33948 (2012).
23. Valcour, V. *et al.* Central nervous system viral invasion and inflammation during acute HIV infection. *J. Infect. Dis.* **206**, 275–282 (2012).
24. Mildvan, D. *et al.* Opportunistic infections and immune deficiency in homosexual men. *Ann. Intern. Med.* **96**, 700–704 (1982).
25. Veazey, R. S. *et al.* Gastrointestinal tract as a major site of CD4+ T cell depletion and viral replication in SIV infection. *Science* **280**, 427–431 (1998).
26. Dion, M.-L. *et al.* HIV infection rapidly induces and maintains a substantial suppression of thymocyte proliferation. *Immunity* **21**, 757–768 (2004).
27. Sun, Y. *et al.* Dysfunction of simian immunodeficiency virus/simian human immunodeficiency virus-induced IL-2 expression by central memory CD4+ T lymphocytes. *J. Immunol.* **174**, 4753–4760 (2005).
28. Zhang, R., Fichtenbaum, C. J., Hildeman, D. A., Lifson, J. D. & Chougnet, C. CD40 ligand dysregulation in HIV infection: HIV glycoprotein 120 inhibits signaling cascades upstream

of CD40 ligand transcription. *J. Immunol.* **172**, 2678–2686 (2004).

29. Herbeuval, J.-P. *et al.* CD4+ T-cell death induced by infectious and noninfectious HIV-1: role of type 1 interferon-dependent, TRAIL/DR5-mediated apoptosis. *Blood* **106**, 3524–3531 (2005).
30. Doitsh, G. *et al.* Cell death by pyroptosis drives CD4 T-cell depletion in HIV-1 infection. *Nature* **505**, 509–514 (2014).
31. Carbonari, M. *et al.* Death of bystander cells by a novel pathway involving early mitochondrial damage in human immunodeficiency virus-related lymphadenopathy. *Blood* **90**, 209–216 (1997).
32. Banda, N. K. *et al.* Crosslinking CD4 by human immunodeficiency virus gp120 primes T cells for activation-induced apoptosis. *J. Exp. Med.* **176**, 1099–1106 (1992).
33. Bartz, S. R. & Emerman, M. Human Immunodeficiency Virus Type 1 Tat Induces Apoptosis and Increases Sensitivity to Apoptotic Signals by Up-Regulating FLICE/Caspase-8. *J. Virol.* **73**, 1956–1963 (1999).
34. Li-Weber, M., Laur, O., Dern, K. & Krammer, P. H. T cell activation-induced and HIV Tat-enhanced CD95(APO-1 / Fas) ligand transcription involves NF-$κ$B. *Eur. J. Immunol.* **30**, (2000).
35. Azad, A. A. Could Nef and Vpr Proteins Contribute to Disease Progression by Promoting Depletion of Bystander Cells and Prolonged Survival of HIV-Infected Cells? *Biochem. Biophys. Res. Commun.* **267**, 677–685 (2000).
36. Badley, A. D. *et al.* Dynamic correlation of apoptosis and immune activation during treatment of HIV infection. *Cell Death Differ.* **6**, 420–432 (1999).
37. Dockrell, D. H. *et al.* Activation-Induced CD4+ T Cell Death in HIV-Positive Individuals Correlates with Fas Susceptibility, CD4+ T Cell Count, and HIV Plasma Viral Copy Number. *AIDS Res. Hum. Retroviruses* **15**, 1509–1518 (1999).
38. Yang, Y., Dong, B., Mittelstadt, P. R., Xiao, H. & Ashwell, J. D. HIV Tat Binds Egr Proteins and Enhances Egr-dependent Transactivation of the Fas Ligand Promoter *. *J. Biol. Chem.* **277**, 19482–19487 (2002).
39. Levy, J. P. Questions about CD8+ anti-HIV lymphocytes in the control of HIV infection.

Antibiot. Chemother. **48**, 13–20 (1996).

40. Day, C. L. *et al.* PD-1 expression on HIV-specific T cells is associated with T-cell exhaustion and disease progression. *Nature* **443**, 350–354 (2006).
41. Andersson, J. *et al.* Low levels of perforin expression in CD8+ T lymphocyte granules in lymphoid tissue during acute human immunodeficiency virus type 1 infection. *J. Infect. Dis.* **185**, 1355–1358 (2002).
42. Fenwick, C. *et al.* T-cell exhaustion in HIV infection. *Immunol. Rev.* **292**, 149–163 (2019).
43. Fuller, M. J. & Zajac, A. J. Ablation of CD8 and CD4 T Cell Responses by High Viral Loads. *J. Immunol.* **170**, 477–486 (2003).
44. Petrovas, C. *et al.* Increased mitochondrial mass characterizes the survival defect of HIV-specific CD8(+) T cells. *Blood* **109**, 2505–2513 (2007).
45. Veiga-Parga, T., Sehrawat, S. & Rouse, B. T. Role of regulatory T cells during virus infection. *Immunol. Rev.* **255**, 182–196 (2013).
46. Yuan, Z. *et al.* HIV-related proteins prolong macrophage survival through induction of Triggering receptor expressed on myeloid cells-1. *Sci. Rep.* **7**, 42028 (2017).
47. Guillemard, E. *et al.* Human immunodeficiency virus 1 favors the persistence of infection by activating macrophages through TNF. *Virology* **329**, 371–380 (2004).
48. Swingler, S., Mann, A. M., Zhou, J., Swingler, C. & Stevenson, M. Apoptotic killing of HIV-1-infected macrophages is subverted by the viral envelope glycoprotein. *PLoS Pathog.* **3**, 1281–1290 (2007).
49. Zheng, L., Yang, Y., Guocai, L., Pauza, C. D. & Salvato, M. S. HIV Tat protein increases Bcl-2 expression in monocytes which inhibits monocyte apoptosis induced by tumor necrosis factor-alpha-related apoptosis-induced ligand. *Intervirology* **50**, 224–228 (2007).
50. Piatak, M. J. *et al.* High levels of HIV-1 in plasma during all stages of infection determined by competitive PCR. *Science* **259**, 1749–1754 (1993).
51. Finzi, D. *et al.* Identification of a reservoir for HIV-1 in patients on highly active antiretroviral therapy. *Science* **278**, 1295–1300 (1997).
52. Speck, S. H. & Ganem, D. Viral latency and its regulation: lessons from the gamma-herpesviruses. *Cell Host Microbe* **8**, 100–115 (2010).

53. Siliciano, J. D. *et al.* Long-term follow-up studies confirm the stability of the latent reservoir for HIV-1 in resting CD4+ T cells. *Nat. Med.* **9**, 727–728 (2003).
54. Siliciano, R. F. & Greene, W. C. HIV latency. *Cold Spring Harb. Perspect. Med.* **1**, 1–19 (2011).
55. Bosque, A. & Planelles, V. Induction of HIV-1 latency and reactivation in primary memory CD4+ T cells. *Blood* **113**, 58–65 (2009).
56. Blankson, J. N., Persaud, D. & Siliciano, R. F. The Challenge of Viral Reservoirs in HIV-1 Infection. *Annu. Rev. Med.* **53**, 557–593 (2002).
57. Eriksson, S. *et al.* Comparative Analysis of Measures of Viral Reservoirs in HIV-1 Eradication Studies. *PLOS Pathog.* **9**, e1003174 (2013).
58. Poon, A. F. Y. *et al.* Quantitation of the latent HIV-1 reservoir from the sequence diversity in viral outgrowth assays. *Retrovirology* **15**, 47 (2018).
59. Descours, B. *et al.* CD32a is a marker of a CD4 T-cell HIV reservoir harbouring replication-competent proviruses. *Nature* **543**, 564–567 (2017).
60. García, M. *et al.* CD32 Expression is not Associated to HIV-DNA content in CD4 cell subsets of individuals with Different Levels of HIV Control. *Sci. Rep.* **8**, 1–8 (2018).
61. Saleh, S. *et al.* Expression and reactivation of HIV in a chemokine induced model of HIV latency in primary resting CD4+ T cells. *Retrovirology* **8**, 80 (2011).
62. Spina, C. A. *et al.* An In-Depth Comparison of Latent HIV-1 Reactivation in Multiple Cell Model Systems and Resting CD4+ T Cells from Aviremic Patients. *PLOS Pathog.* **9**, e1003834 (2013).
63. Lassen, K. G., Hebbeler, A. M., Bhattacharyya, D., Lobritz, M. A. & Greene, W. C. A flexible model of HIV-1 latency permitting evaluation of many primary CD4 T-cell reservoirs. *PLoS One* **7**, e30176 (2012).
64. Jordan, A., Bisgrove, D. & Verdin, E. HIV reproducibly establishes a latent infection after acute infection of T cells in vitro. *EMBO J.* **22**, 1868–1877 (2003).
65. Yefei, H. *et al.* Resting CD4+ T Cells from Human Immunodeficiency Virus Type 1 (HIV-1)-Infected Individuals Carry Integrated HIV-1 Genomes within Actively Transcribed Host Genes. *J. Virol.* **78**, 6122–6133 (2004).

66. Blazkova, J. *et al.* CpG methylation controls reactivation of HIV from latency. *PLoS Pathog.* **5**, e1000554 (2009).
67. Kauder, S. E., Bosque, A., Lindqvist, A., Planelles, V. & Verdin, E. Epigenetic regulation of HIV-1 latency by cytosine methylation. *PLoS Pathog.* **5**, e1000495 (2009).
68. Aquaro, S. *et al.* Long-term survival and virus production in human primary macrophages infected by human immunodeficiency virus. *J. Med. Virol.* **68**, 479–488 (2002).
69. Chun, T. W. *et al.* Relationship between pre-existing viral reservoirs and the re-emergence of plasma viremia after discontinuation of highly active anti-retroviral therapy. *Nat. Med.* **6**, 757–761 (2000).
70. Honeycutt, J. B. *et al.* HIV persistence in tissue macrophages of humanized myeloid-only mice during antiretroviral therapy. *Nat. Med.* **23**, 638–643 (2017).
71. Chandrasekar, A. P. The Role of the BCL-2 Family of Proteins in HIV-1. **33**, 1–25 (2020).
72. Aillet, F. *et al.* Human immunodeficiency virus induces a dual regulation of Bcl-2, resulting in persistent infection of CD4(+) T- or monocytic cell lines. *J. Virol.* **72**, 9698–9705 (1998).
73. Guillemard, E. *et al.* Human immunodeficiency virus 1 favors the persistence of infection by activating macrophages through TNF. *Virology* **329**, 371–380 (2004).
74. Busca, A., Saxena, M. & Kumar, A. Critical role for antiapoptotic Bcl-xL and Mcl-1 in human macrophage survival and cellular IAP1/2 (cIAP1/2) in resistance to HIV-Vpr-induced apoptosis. *J. Biol. Chem.* **287**, 15118–15133 (2012).
75. Zhu, Y., Roshal, M., Li, F., Blackett, J. & Planelles, V. Upregulation of survivin by HIV-1 Vpr. *Apoptosis* **8**, 71–79 (2003).
76. Cassol, E., Alfano, M., Biswas, P. & Poli, G. Monocyte-derived macrophages and myeloid cell lines as targets of HIV-1 replication and persistence. *J. Leukoc. Biol.* **80**, 1018–1030 (2006).
77. Réu, P. *et al.* The Lifespan and Turnover of Microglia in the Human Brain. *Cell Rep.* **20**, 779–784 (2017).
78. Cenker, J. J., Stultz, R. D. & McDonald, D. Brain Microglial Cells Are Highly Susceptible to HIV-1 Infection and Spread. *AIDS Res. Hum. Retroviruses* **33**, 1155–1165 (2017).

79. Foley, J. F. *et al.* Roles for CXC chemokine ligands 10 and 11 in recruiting CD4+ T cells to HIV-1-infected monocyte-derived macrophages, dendritic cells, and lymph nodes. *J. Immunol.* **174**, 4892–4900 (2005).
80. Groot, F., Welsch, S. & Sattentau, Q. J. Efficient HIV-1 transmission from macrophages to T cells across transient virological synapses. *Blood* **111**, 4660–4663 (2008).
81. Lopes, J. R., Chiba, D. E. & Dos Santos, J. L. HIV latency reversal agents: A potential path for functional cure? *Eur. J. Med. Chem.* **213**, 113213 (2021).
82. Bertrand, P. Inside HDAC with HDAC inhibitors. *Eur. J. Med. Chem.* **45**, 2095–2116 (2010).
83. Archin, N. M. *et al.* Erratum: Administration of vorinostat disrupts HIV-1 latency in patients on antiretroviral therapy. *Nature* **489**, 460 (2012).
84. Archin, N. M. *et al.* Interval dosing with the HDAC inhibitor vorinostat effectively reverses HIV latency. *J. Clin. Invest.* **127**, 3126–3135 (2017).
85. Marsden, M. D. *et al.* Characterization of designed, synthetically accessible bryostatin analog HIV latency reversing agents. *Virology* **520**, 83–93 (2018).
86. Zhu, J. *et al.* Reactivation of latent HIV-1 by inhibition of BRD4. *Cell Rep.* **2**, 807–816 (2012).
87. Williams, S. A. *et al.* Prostratin Antagonizes HIV Latency by Activating NF-κB*. *J. Biol. Chem.* **279**, 42008–42017 (2004).
88. Gutiérrez, C. *et al.* Bryostatin-1 for latent virus reactivation in HIV-infected patients on antiretroviral therapy. *AIDS* **30**, (2016).
89. Schlaepfer, E., Audigé, A., Joller, H. & Speck, R. F. TLR7/8 Triggering Exerts Opposing Effects in Acute versus Latent HIV Infection. *J. Immunol.* **176**, 2888–2895 (2006).
90. Rasmus, O. *et al.* A Novel Toll-Like Receptor 9 Agonist, MGN1703, Enhances HIV-1 Transcription and NK Cell-Mediated Inhibition of HIV-1-Infected Autologous CD4+ T Cells. *J. Virol.* **90**, 4441–4453 (2016).
91. López-Huertas, M. R. *et al.* The CCR5-antagonist Maraviroc reverses HIV-1 latency in vitro alone or in combination with the PKC-agonist Bryostatin-1. *Sci. Rep.* **7**, 2385 (2017).
92. Stephenson, K. E. Therapeutic vaccination for HIV: Hopes and challenges. *Curr. Opin. HIV AIDS* **13**, 408–415 (2018).

93. García, F. *et al.* A therapeutic dendritic cell-based vaccine for HIV-1 infection. *J. Infect. Dis.* **203 4**, 473–478 (2011).
94. Lévy, Y. *et al.* Immunological and virological efficacy of a therapeutic immunization combined with interleukin-2 in chronically HIV-1 infected patients. *AIDS* **19**, 279–286 (2005).
95. Lévy, Y. *et al.* Sustained control of viremia following therapeutic immunization in chronically HIV-1-infected individuals. *AIDS* **20**, 405–413 (2006).
96. Kim, Y., Anderson, J. L. & Lewin, S. R. Getting the 'Kill' into 'Shock and Kill': Strategies to Eliminate Latent HIV. *Cell Host Microbe* **23**, 14–26 (2018).
97. Hütter, G. *et al.* Long-term control of HIV by CCR5 Delta32/Delta32 stem-cell transplantation. *N. Engl. J. Med.* **360**, 692–698 (2009).
98. Liu, R. *et al.* Homozygous Defect in HIV-1 Coreceptor Accounts for Resistance of Some Multiply-Exposed Individuals to HIV-1 Infection. *Cell* **86**, 367–377 (1996).
99. Allen, A. G. *et al.* Gene Editing of HIV-1 Co-receptors to Prevent and/or Cure Virus Infection. *Front. Microbiol.* **9**, 1–14 (2018).
100. Urnov, F. D. *et al.* Highly efficient endogenous human gene correction using designed zinc-finger nucleases. *Nature* **435**, 646–651 (2005).
101. Perez, E. E. *et al.* Establishment of HIV-1 resistance in CD4+ T cells by genome editing using zinc-finger nucleases. *Nat. Biotechnol.* **26**, 808–816 (2008).
102. Holt, N. *et al.* Human hematopoietic stem/progenitor cells modified by zinc-finger nucleases targeted to CCR5 control HIV-1 in vivo. *Nat. Biotechnol.* **28**, 839–847 (2010).
103. Khalili, K., White, M. K. & Jacobson, J. M. Novel AIDS therapies based on gene editing. *Cell. Mol. Life Sci.* **74**, 2439–2450 (2017).
104. Mussolino, C. *et al.* A novel TALE nuclease scaffold enables high genome editing activity in combination with low toxicity. *Nucleic Acids Res.* **39**, 9283–9293 (2011).
105. Yu Qing, A. *et al.* TALENs-mediated homozygous CCR5Δ32 mutations endow CD4+ U87 cells with resistance against HIV-1 infection. *Mol Med Rep* **17**, 243–249 (2018).
106. Yu, S. *et al.* Simultaneous Knockout of CXCR4 and CCR5 Genes in CD4+ T Cells via CRISPR/Cas9 Confers Resistance to Both X4- and R5-Tropic Human Immunodeficiency

Virus Type 1 Infection. *Hum. Gene Ther.* **29**, 51–67 (2017).

107. Bella, R. *et al.* Removal of HIV DNA by CRISPR from Patient Blood Engrafts in Humanized Mice. *Mol. Ther. Nucleic Acids* **12**, 275–282 (2018).
108. Hiatt, J. *et al.* A functional map of HIV-host interactions in primary human T cells. *Nat. Commun.* **13**, 1752 (2022).
109. Vansant, G., Bruggemans, A., Janssens, J. & Debyser, Z. Block-And-Lock Strategies to Cure HIV Infection. *Viruses* **12**, (2020).
110. Rice, A. P. The HIV-1 Tat Protein: Mechanism of Action and Target for HIV-1 Cure Strategies. *Curr. Pharm. Des.* **23**, 4098–4102 (2017).
111. Mousseau, G. *et al.* An analog of the natural steroidal alkaloid cortistatin A potently suppresses Tat-dependent HIV transcription. *Cell Host Microbe* **12**, 97–108 (2012).
112. Mousseau, G. *et al.* The Tat Inhibitor Didehydro-Cortistatin A Prevents HIV-1 Reactivation from Latency. *MBio* **6**, e00465 (2015).
113. Kessing, C. F. *et al.* In Vivo Suppression of HIV Rebound by Didehydro-Cortistatin A, a 'Block-and-Lock' Strategy for HIV-1 Treatment. *Cell Rep.* **21**, 600–611 (2017).
114. Christ, F. *et al.* Small-molecule inhibitors of the LEDGF/p75 binding site of integrase block HIV replication and modulate integrase multimerization. *Antimicrob. Agents Chemother.* **56**, 4365–4374 (2012).
115. Balakrishnan, M. *et al.* Non-catalytic site HIV-1 integrase inhibitors disrupt core maturation and induce a reverse transcription block in target cells. *PLoS One* **8**, e74163 (2013).
116. Desimmie, B. A. *et al.* LEDGINs inhibit late stage HIV-1 replication by modulating integrase multimerization in the virions. *Retrovirology* **10**, 57 (2013).
117. Debyser, Z., Vansant, G., Bruggemans, A., Janssens, J. & Christ, F. Insight in HIV Integration Site Selection Provides a Block-and-Lock Strategy for a Functional Cure of HIV Infection. *Viruses* **11**, (2018).
118. Suzuki, K. *et al.* Closed chromatin architecture is induced by an RNA duplex targeting the HIV-1 promoter region. *J. Biol. Chem.* **283**, 23353–23363 (2008).
119. Ahlenstiel, C. *et al.* Novel RNA Duplex Locks HIV-1 in a Latent State via Chromatin-

mediated Transcriptional Silencing. *Mol. Ther. Nucleic Acids* **4**, e261 (2015).

120. Naik, S. & Russell, S. J. Engineering oncolytic viruses to exploit tumor specific defects in innate immune signaling pathways. *Expert Opin. Biol. Ther.* **9**, 1163–1176 (2009).
121. Rahman, M. M. & McFadden, G. Oncolytic viruses: Newest frontier for cancer immunotherapy. *Cancers (Basel).* **13**, (2021).
122. Alberts, P., Tilgase, A., Rasa, A., Bandere, K. & Venskus, D. The advent of oncolytic virotherapy in oncology: The Rigvir® story. *Eur. J. Pharmacol.* **837**, 117–126 (2018).
123. Wei, D., Xu, J., Liu, X.-Y., Chen, Z.-N. & Bian, H. Fighting Cancer with Viruses: Oncolytic Virus Therapy in China. *Hum. Gene Ther.* **29**, 151–159 (2018).
124. Raman, S. S., Hecht, J. R. & Chan, E. Talimogene laherparepvec: review of its mechanism of action and clinical efficacy and safety. *Immunotherapy* **11**, 705–723 (2019).
125. Sugawara, K. *et al.* Oncolytic herpes virus G47Δ works synergistically with CTLA-4 inhibition via dynamic intratumoral immune modulation. *Mol. Ther. oncolytics* **22**, 129–142 (2021).
126. Harrington, K., Freeman, D. J., Kelly, B., Harper, J. & Soria, J.-C. Optimizing oncolytic virotherapy in cancer treatment. *Nat. Rev. Drug Discov.* **18**, 689–706 (2019).
127. Lawler, S. E., Speranza, M.-C., Cho, C.-F. & Chiocca, E. A. Oncolytic Viruses in Cancer Treatment: A Review. *JAMA Oncol.* **3**, 841–849 (2017).
128. Zainutdinov, S. S., Kochneva, G. V, Netesov, S. V, Chumakov, P. M. & Matveeva, O. V. Directed evolution as a tool for the selection of oncolytic RNA viruses with desired phenotypes. *Oncolytic virotherapy* **8**, 9–26 (2019).
129. He, Y. *et al.* Complexes of poliovirus serotypes with their common cellular receptor, CD155. *J. Virol.* **77**, 4827–4835 (2003).
130. Anderson, B. D., Nakamura, T., Russell, S. J. & Peng, K.-W. High CD46 receptor density determines preferential killing of tumor cells by oncolytic measles virus. *Cancer Res.* **64**, 4919–4926 (2004).
131. Bergelson, J. M., Shepley, M. P., Chan, B. M., Hemler, M. E. & Finberg, R. W. Identification of the integrin VLA-2 as a receptor for echovirus 1. *Science* **255**, 1718–1720 (1992).
132. Yu, Z. *et al.* Nectin-1 expression by squamous cell carcinoma is a predictor of herpes

oncolytic sensitivity. *Mol. Ther.* **15**, 103–113 (2007).

133. Takaoka, A., Tamura, T. & Taniguchi, T. Interferon regulatory factor family of transcription factors and regulation of oncogenesis. *Cancer Sci.* **99**, 467–478 (2008).
134. Berchtold, S. *et al.* Innate immune defense defines susceptibility of sarcoma cells to measles vaccine virus-based oncolysis. *J. Virol.* **87**, 3484–3501 (2013).
135. Stojdl, D. F. *et al.* Exploiting tumor-specific defects in the interferon pathway with a previously unknown oncolytic virus. *Nat. Med.* **6**, 821–825 (2000).
136. Brun, J. *et al.* Identification of genetically modified maraba virus as an oncolytic rhabdovirus. *Mol. Ther.* **18**, 1440–1449 (2010).
137. Pol, J. G. *et al.* Maraba virus as a potent oncolytic vaccine vector. *Mol. Ther.* **22**, 420–429 (2014).
138. Stojdl, D. F. *et al.* VSV strains with defects in their ability to shutdown innate immunity are potent systemic anti-cancer agents. *Cancer Cell* **4**, 263–275 (2003).
139. Balachandran, S. & Barber, G. N. Vesicular stomatitis virus (VSV) therapy of tumors. *IUBMB Life* **50**, 135–138 (2000).
140. Atherton, M. J. *et al.* Customized viral immunotherapy for HPV-associated cancer. *Cancer Immunol. Res.* **5**, 847–859 (2017).
141. Bourgeois-Daigneault, M. C. *et al.* Combination of Paclitaxel and MG1 oncolytic virus as a successful strategy for breast cancer treatment. *Breast Cancer Res.* **18**, 1–10 (2016).
142. Hummel, J. *et al.* Maraba virus-vectored cancer vaccines represent a safe and novel therapeutic option for cats. *Sci. Rep.* **7**, 1–12 (2017).
143. Pol, J. *et al.* Development and applications of oncolytic Maraba virus vaccines. *Oncolytic Virotherapy* **Volume 7**, 117–128 (2018).
144. Doehle, B. P., Hladik, F., McNevin, J. P., McElrath, M. J. & Gale, M. J. Human immunodeficiency virus type 1 mediates global disruption of innate antiviral signaling and immune defenses within infected cells. *J. Virol.* **83**, 10395–10405 (2009).
145. Solis, M. *et al.* RIG-I-mediated antiviral signaling is inhibited in HIV-1 infection by a protease-mediated sequestration of RIG-I. *J. Virol.* **85**, 1224–1236 (2011).
146. Clerzius, G., Gélinas, J.-F. & Gatignol, A. Multiple levels of PKR inhibition during HIV-1

replication. *Rev. Med. Virol.* **21**, 42–53 (2011).

147. Foster, J. L., Denial, S. J., Temple, B. R. S. & Garcia, J. V. Mechanisms of HIV-1 Nef function and intracellular signaling. *J. neuroimmune Pharmacol. Off. J. Soc. NeuroImmune Pharmacol.* **6**, 230–246 (2011).
148. Ranganath, N., Sandstrom, T. S., Schinkel, S. C. B., Côté, S. C. & Angel, J. B. The oncolytic virus MG1 targets and eliminates cells latently infected with HIV-1: Implications for an HIV cure. *J. Infect. Dis.* **217**, 721–730 (2018).
149. Sandstrom, T. S. *et al.* HIV-Infected Macrophages Are Infected and Killed by the Interferon-Sensitive Rhabdovirus MG1. *J. Virol.* **95**, 1–18 (2021).
150. Kerr, J. F., Wyllie, A. H. & Currie, A. R. Apoptosis: a basic biological phenomenon with wide-ranging implications in tissue kinetics. *Br. J. Cancer* **26**, 239–257 (1972).
151. McIlwain, D. R., Berger, T. & Mak, T. W. Caspase functions in cell death and disease. *Cold Spring Harb. Perspect. Biol.* **5**, 1–28 (2013).
152. Nagata, S. Apoptosis and Clearance of Apoptotic Cells. *Annu. Rev. Immunol.* **36**, 489–517 (2018).
153. Elmore, S. Apoptosis: A Review of Programmed Cell Death. *Toxicol. Pathol.* **35**, 495–516 (2007).
154. Brunner, T. *et al.* Fas (CD95/Apo-1) ligand regulation in T cell homeostasis, cell-mediated cytotoxicity and immune pathology. *Semin. Immunol.* **15**, 167–176 (2003).
155. Enari, M. *et al.* A caspase-activated DNase that degrades DNA during apoptosis, and its inhibitor ICAD. *Nature* **391**, 43–50 (1998).
156. Baize, S. *et al.* Inflammatory responses in Ebola virus-infected patients. *Clin. Exp. Immunol.* **128**, 163–168 (2002).
157. Gannagé, M. *et al.* Matrix protein 2 of influenza A virus blocks autophagosome fusion with lysosomes. *Cell Host Microbe* **6**, 367–380 (2009).
158. Strack, P. R. *et al.* Apoptosis mediated by HIV protease is preceded by cleavage of Bcl-2. *Proc. Natl. Acad. Sci. U. S. A.* **93**, 9571–9576 (1996).
159. Nagata, S. & Tanaka, M. Programmed cell death and the immune system. *Nat. Rev. Immunol.* **17**, 333–340 (2017).

160. Miao, E. A. *et al.* Caspase-1-induced pyroptosis is an innate immune effector mechanism against intracellular bacteria. *Nat. Immunol.* **11**, 1136–1142 (2010).
161. Fernandes-Alnemri, T., Yu, J.-W., Datta, P., Wu, J. & Alnemri, E. S. AIM2 activates the inflammasome and cell death in response to cytoplasmic DNA. *Nature* **458**, 509–513 (2009).
162. Shi, J., Gao, W. & Shao, F. Pyroptosis: Gasdermin-Mediated Programmed Necrotic Cell Death. *Trends Biochem. Sci.* **42**, 245–254 (2017).
163. Lawrence, T. M., Hudacek, A. W., de Zoete, M. R., Flavell, R. A. & Schnell, M. J. Rabies virus is recognized by the NLRP3 inflammasome and activates interleukin-1β release in murine dendritic cells. *J. Virol.* **87**, 5848–5857 (2013).
164. Kofahi, H. M., Taylor, N. G. A., Hirasawa, K., Grant, M. D. & Russell, R. S. Hepatitis C Virus Infection of Cultured Human Hepatoma Cells Causes Apoptosis and Pyroptosis in Both Infected and Bystander Cells. *Sci. Rep.* **6**, 37433 (2016).
165. Thomas, P. G. *et al.* The intracellular sensor NLRP3 mediates key innate and healing responses to influenza A virus via the regulation of caspase-1. *Immunity* **30**, 566–575 (2009).
166. Zhao, J. *et al.* Mixed lineage kinase domain-like is a key receptor interacting protein 3 downstream component of TNF-induced necrosis. *Proc. Natl. Acad. Sci. U. S. A.* **109**, 5322–5327 (2012).
167. Sun, L. *et al.* Mixed lineage kinase domain-like protein mediates necrosis signaling downstream of RIP3 kinase. *Cell* **148**, 213–227 (2012).
168. Berghe, T. Vanden, Linkermann, A., Jouan-Lanhouet, S., Walczak, H. & Vandenabeele, P. Regulated necrosis: The expanding network of non-apoptotic cell death pathways. *Nat. Rev. Mol. Cell Biol.* **15**, 135–147 (2014).
169. Oberst, A. *et al.* Catalytic activity of the caspase-8-FLIP(L) complex inhibits RIPK3-dependent necrosis. *Nature* **471**, 363–367 (2011).
170. Holler, N. *et al.* Fas triggers an alternative, caspase-8-independent cell death pathway using the kinase RIP as effector molecule. *Nat. Immunol.* **1**, 489–495 (2000).
171. Vandenabeele, P., Galluzzi, L., Vanden Berghe, T. & Kroemer, G. Molecular mechanisms

of necroptosis: An ordered cellular explosion. *Nat. Rev. Mol. Cell Biol.* **11**, 700–714 (2010).

172. Wang, H. *et al.* Mixed lineage kinase domain-like protein MLKL causes necrotic membrane disruption upon phosphorylation by RIP3. *Mol. Cell* **54**, 133–146 (2014).
173. Gaiha, G. D. *et al.* Dysfunctional HIV-specific CD8+ T cell proliferation is associated with increased caspase-8 activity and mediated by necroptosis. *Immunity* **41**, 1001–1012 (2014).
174. Cho, Y. S. *et al.* Phosphorylation-driven assembly of the RIP1-RIP3 complex regulates programmed necrosis and virus-induced inflammation. *Cell* **137**, 1112–1123 (2009).
175. Butera, S. T. *et al.* Extrachromosomal human immunodeficiency virus type-1 DNA can initiate a spreading infection of HL-60 cells. *J. Cell. Biochem.* **45**, 366–373 (1991).
176. Perez, V. L. *et al.* An HIV-1-infected T cell clone defective in IL-2 production and Ca2+ mobilization after CD3 stimulation. *J. Immunol.* **147**, 3145–3148 (1991).
177. Bernabei, P. *et al.* Interferon-γ receptor 2 expression as the deciding factor in human T, B, and myeloid cell proliferation or death. *J. Leukoc. Biol.* **70**, 950–960 (2001).
178. Ranganath, N., Sandstrom, T. S., Fadel, S., Côté, S. C. & Angel, J. B. Type I interferon responses are impaired in latently HIV infected cells. *Retrovirology* **13**, 1–9 (2016).
179. Harman, A. N. *et al.* HIV Blocks Interferon Induction in Human Dendritic Cells and Macrophages by Dysregulation of TBK1. *J. Virol.* **89**, 6575–6584 (2015).
180. Lau, A. S., Read, S. E. & Williams, B. R. Downregulation of interferon alpha but not gamma receptor expression in vivo in the acquired immunodeficiency syndrome. *J. Clin. Invest.* **82**, 1415–1421 (1988).
181. Akhtar, L. N. *et al.* Suppressor of cytokine signaling 3 inhibits antiviral IFN-beta signaling to enhance HIV-1 replication in macrophages. *J. Immunol.* **185**, 2393–2404 (2010).
182. Mocarski, E. S., Upton, J. W. & Kaiser, W. J. Viral infection and the evolution of caspase 8-regulated apoptotic and necrotic death pathways. *Nat. Rev. Immunol.* **12**, 79–88 (2011).
183. Lam, W. Y. *et al.* Avian influenza virus A/HK/483/97(H5N1) NS1 protein induces apoptosis in human airway epithelial cells. *J. Virol.* **82**, 2741–2751 (2008).
184. Tripathi, S. *et al.* Influenza A virus nucleoprotein induces apoptosis in human airway

epithelial cells: implications of a novel interaction between nucleoprotein and host protein Clusterin. *Cell Death Dis.* **4**, e562 (2013).

185. Hartmann, B. M. *et al.* Pandemic H1N1 influenza A viruses suppress immunogenic RIPK3-driven dendritic cell death. *Nat. Commun.* **8**, 1931 (2017).
186. Jorgensen, I., Rayamajhi, M. & Miao, E. A. Programmed cell death as a defence against infection. *Nat. Rev. Immunol.* **17**, 151–164 (2017).
187. Kuriakose, T. *et al.* ZBP1/DAI is an innate sensor of influenza virus triggering the NLRP3 inflammasome and programmed cell death pathways. *Sci. Immunol.* **1**, (2016).
188. Chang, P. *et al.* Early apoptosis of porcine alveolar macrophages limits avian influenza virus replication and pro-inflammatory dysregulation. *Sci. Rep.* **5**, 17999 (2015).
189. Chen, W. *et al.* A novel influenza A virus mitochondrial protein that induces cell death. *Nat. Med.* **7**, 1306–1312 (2001).
190. Liu, Y. *et al.* Cell-Type Apoptosis in Lung during SARS-CoV-2 Infection. *Pathog. (Basel, Switzerland)* **10**, (2021).
191. Li, J. *et al.* Insight to Pyroptosis in Viral Infectious Diseases. *Health (Irvine. Calif).* **13**, 574–590 (2021).
192. Douzandegan, Y. *et al.* Cell Death Mechanisms in Esophageal Squamous Cell Carcinoma Induced by Vesicular Stomatitis Virus Matrix Protein. *Osong public Heal. Res. Perspect.* **10**, 246–252 (2019).
193. Rajan, J. V, Rodriguez, D., Miao, E. A. & Aderem, A. The NLRP3 inflammasome detects encephalomyocarditis virus and vesicular stomatitis virus infection. *J. Virol.* **85**, 4167–4172 (2011).
194. Bolton, D. L. *et al.* Death of CD4 + T-Cell Lines Caused by Human Immunodeficiency Virus Type 1 Does Not Depend on Caspases or Apoptosis . *J. Virol.* **76**, 5094–5107 (2002).
195. Connolly, P. F. & Fearnhead, H. O. Viral hijacking of host caspases: An emerging category of pathogen-host interactions. *Cell Death Differ.* **24**, 1401–1410 (2017).
196. Callus, B. A. & Vaux, D. L. Caspase inhibitors: viral, cellular and chemical. *Cell Death Differ.* **14**, 73–78 (2007).
197. J., C. R., Marcus, F. & K., M. L. Prevention of Apoptosis by a Baculovirus Gene During

Infection of Insect Cells. *Science (80-.).* **254**, 1388–1390 (1991).

198. Izquierdo, M. *et al.* Blocked negative selection of developing T cells in mice expressing the baculovirus p35 caspase inhibitor. *EMBO J.* **18**, 156–166 (1999).
199. Galvan, V., Brandimarti, R. & Roizman, B. Herpes Simplex Virus 1 Blocks Caspase-3-Independent and Caspase-Dependent Pathways to Cell Death. *J. Virol.* **73**, 3219–3226 (1999).
200. Mack, C., Sickmann, A., Lembo, D. & Brune, W. Inhibition of proinflammatory and innate immune signaling pathways by a cytomegalovirus RIP1-interacting protein. *Proc. Natl. Acad. Sci. U. S. A.* **105**, 3094–3099 (2008).
201. Kettle, S. *et al.* Vaccinia virus serpin B13R (SPI-2) inhibits interleukin-1beta-converting enzyme and protects virus-infected cells from TNF- and Fas-mediated apoptosis, but does not prevent IL-1beta-induced fever. *J. Gen. Virol.* **78 (Pt 3)**, 677–685 (1997).
202. Cai, R. *et al.* Caspase-1 Activity in CD4 T Cells Is Downregulated Following Antiretroviral Therapy for HIV-1 Infection. *AIDS Res. Hum. Retroviruses* **33**, 164–171 (2016).
203. Pan, T. *et al.* Necroptosis takes place in human immunodeficiency virus type-1 (HIV-1)-infected CD4+ T lymphocytes. *PLoS One* **9**, e93944–e93944 (2014).
204. Terahara, K., Iwabuchi, R., Iwaki, R., Takahashi, Y. & Tsunetsugu-Yokota, Y. Substantial induction of non-apoptotic CD4 T-cell death during the early phase of HIV-1 infection in a humanized mouse model. *Microbes Infect.* **23**, 104767 (2021).
205. Fernández Larrosa, P. N. *et al.* Apoptosis resistance in HIV-1 persistently-infected cells is independent of active viral replication and involves modulation of the apoptotic mitochondrial pathway. *Retrovirology* **5**, 1–12 (2008).
206. Tanaka, Y. *et al.* Establishment of persistent infection with HIV-1 abrogates the caspase-3-dependent apoptotic signaling pathway in U937 cells. *Exp. Cell Res.* **247**, 514–524 (1999).
207. Gioia, L., Siddique, A., Head, S. R., Salomon, D. R. & Su, A. I. A genome-wide survey of mutations in the Jurkat cell line. *BMC Genomics* **19**, 334 (2018).
208. Kulawiec, M., Owens, K. M. & Singh, K. K. Cancer cell mitochondria confer apoptosis resistance and promote metastasis. *Cancer Biol. Ther.* **8**, 1378–1385 (2009).

209. Sandstrom, T. Impairment of type 1 interferon response in HIV-infected macrophages facilitates their infection and killing by the oncolytic maraba virus, MG1 (2019).

Appendix A

Supplementary Data

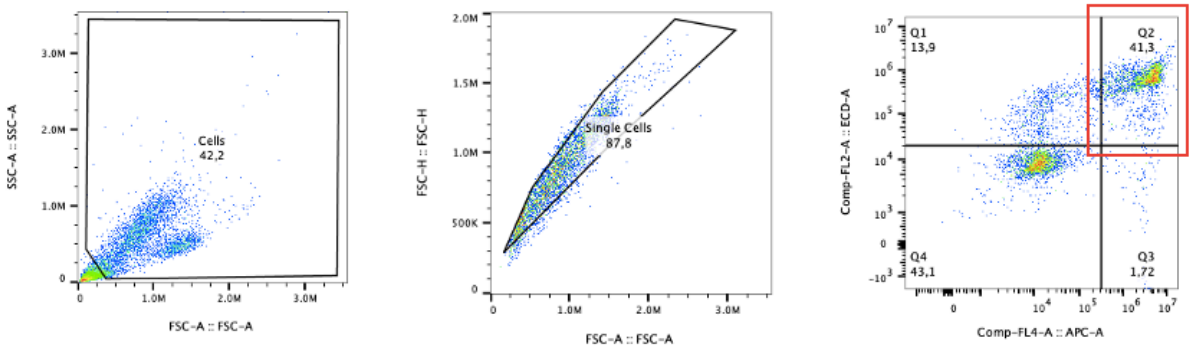

Supplementary Figure 1. Gating strategy for cell death experiments using caspase inhibitors. A bulk cell gate is placed to exclude debris while still incorporating dead cells. Single cells are gated to exclude duplets, and APC (AnnexinV) vs. PI (ECD) graphs are generated, gating on the double positive population to include apoptotic cells.

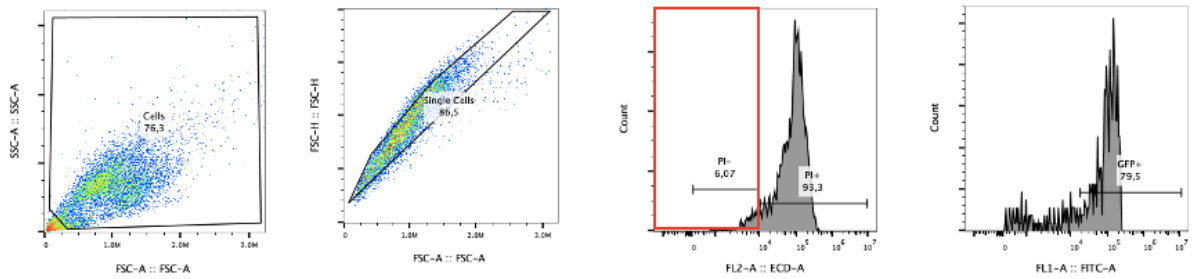

Supplementary Figure 2. Gating strategy for MG1 dose response experiments. A bulk cell gate is placed to include dead cells, followed by a single cell gate to exclude duplets. The PI negative (PI-) population is gated on to include the live cells, followed by a gate for eGFP. An infected cells is described as a live cell (i.e PI-) expressing eGFP.

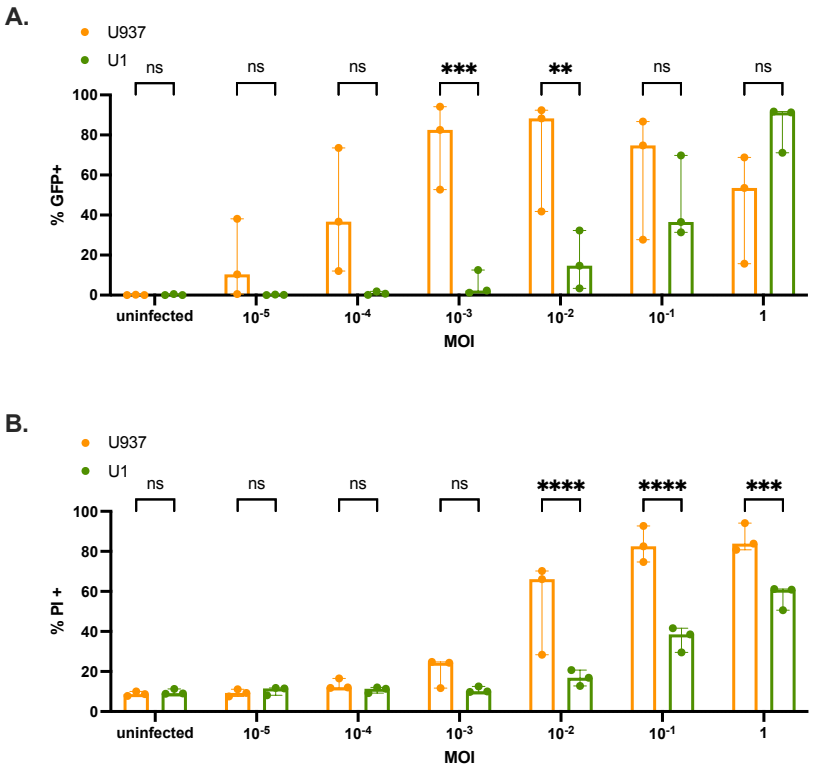

Supplementary Figure 3. MG1 dose response on healthy U937 cells and HIV infected U1 cells. Cells were infected with MG1 at MOI 10^{-5} to MOI 1 for 24 hours and flow cytometry was performed, reading eGFP **(A)** and PI **(B)**. Two – way ANOVA with multiple comparisons test (n = 3). ** = p – value < 0.01, *** = p – value < 0.001, and **** = p – value < 0.0001.

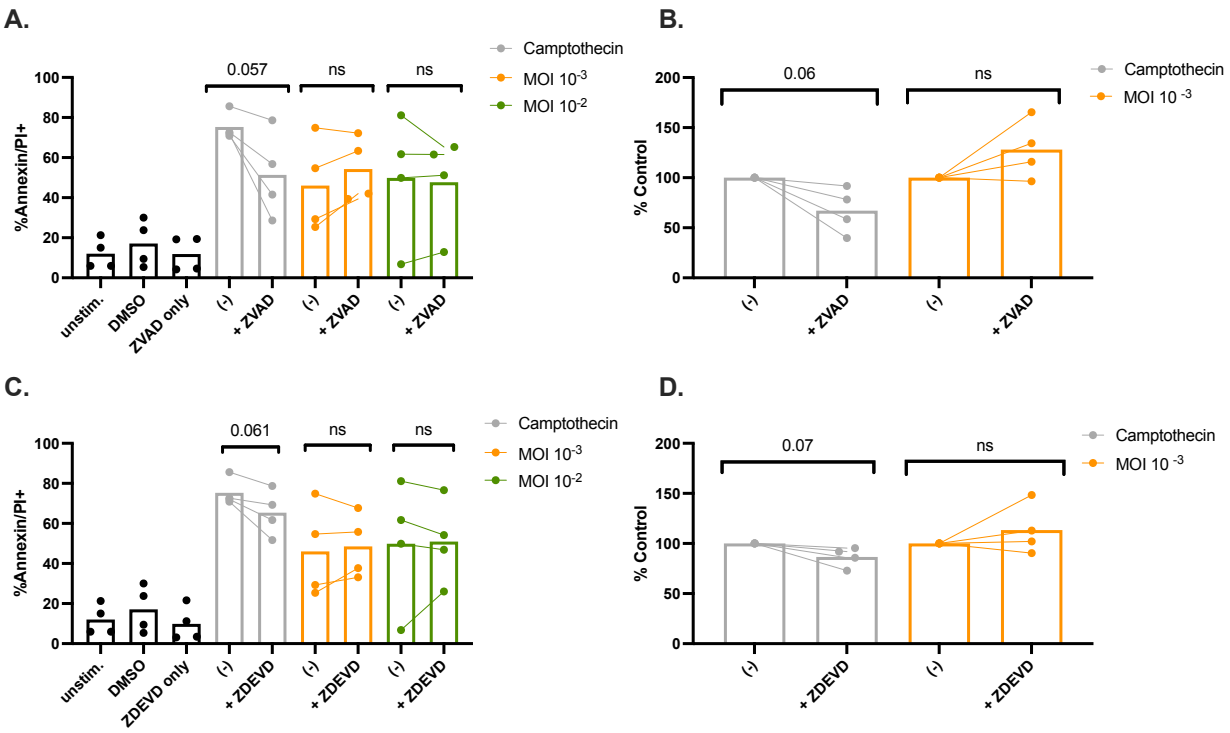

Supplementary Figure 4. MG1 infection of healthy U937 cells in the presence of the caspase inhibitors Z-VAD-FMK (A) and Z-DEVD-FMK (C). Cells were pre – treated for 1 hour with 50uM of either caspase inhibitor, after which they were infected with MG1 at MOI 10^{-3} or MOI 10^{-2}. After 24 hours, cell death was analyzed using flow cytometry, staining for AnnexinV and PI. Camptothecin (10uM) was used a positive control for cell death. Data in comparison to the control is depicted in **B** and **D**. Students T test performed (n = 4).

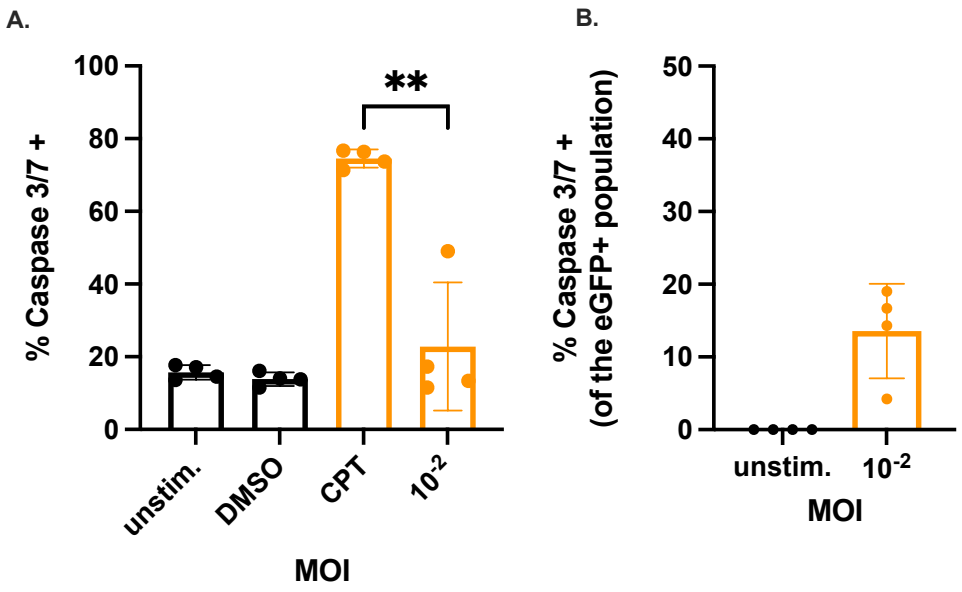

Supplementary Figure 5. Caspase activity during MG1 infection of healthy U937 cells. Cells were infected with MG1 at MOI 10^{-2} for 24 hours. FLICA 660 caspase 3/7 staining was performed, and cells were analyzed using flow cytometry. Camptothecin (10uM) was used as a positive control for caspase activity. Bulk caspase activity (**A**) and caspase activity during MG1 infection (**B**) is shown. Gating strategy is described in **Figures 10A, C and 11A, C.**

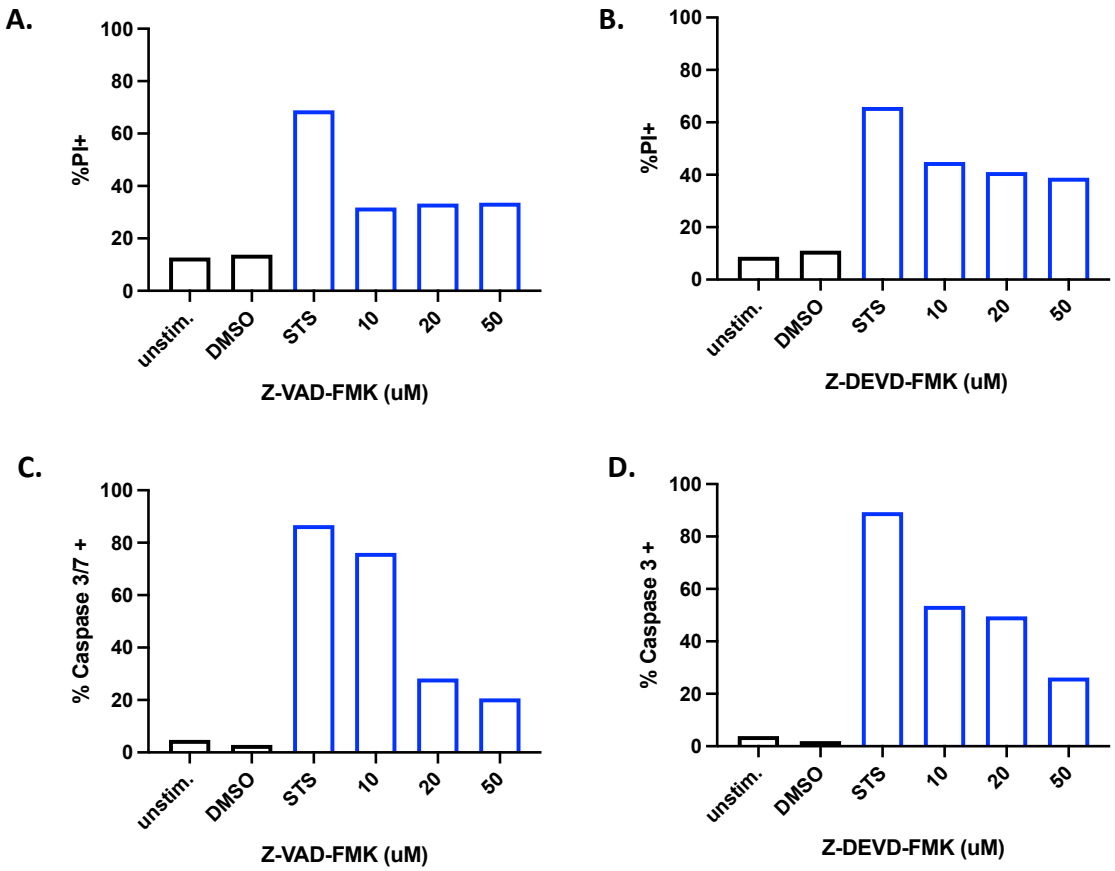

Supplementary Figure 6. Z- VAD-FMK and Z-DEVD-FMK optimizations on Jurkat cells. Cells were pre – treated for 1 hour with 10, 20, 50uM of either inhibitor, or left unstimulated. DMSO was used as a vehicle control. After 1 hour, 2uM Staurosporine was added to induce apoptosis. Following a 24-hour incubation, cells were stained with either PI (**A, B**), FLICA 660 caspase 3/7 stain (**C**), or an anti – active caspase 3 APC conjugated antibody (BD Biosciences # 560626, **D**). Cell death or caspase activity was analyzed using flow cytometry. No statistics performed (n = 1).

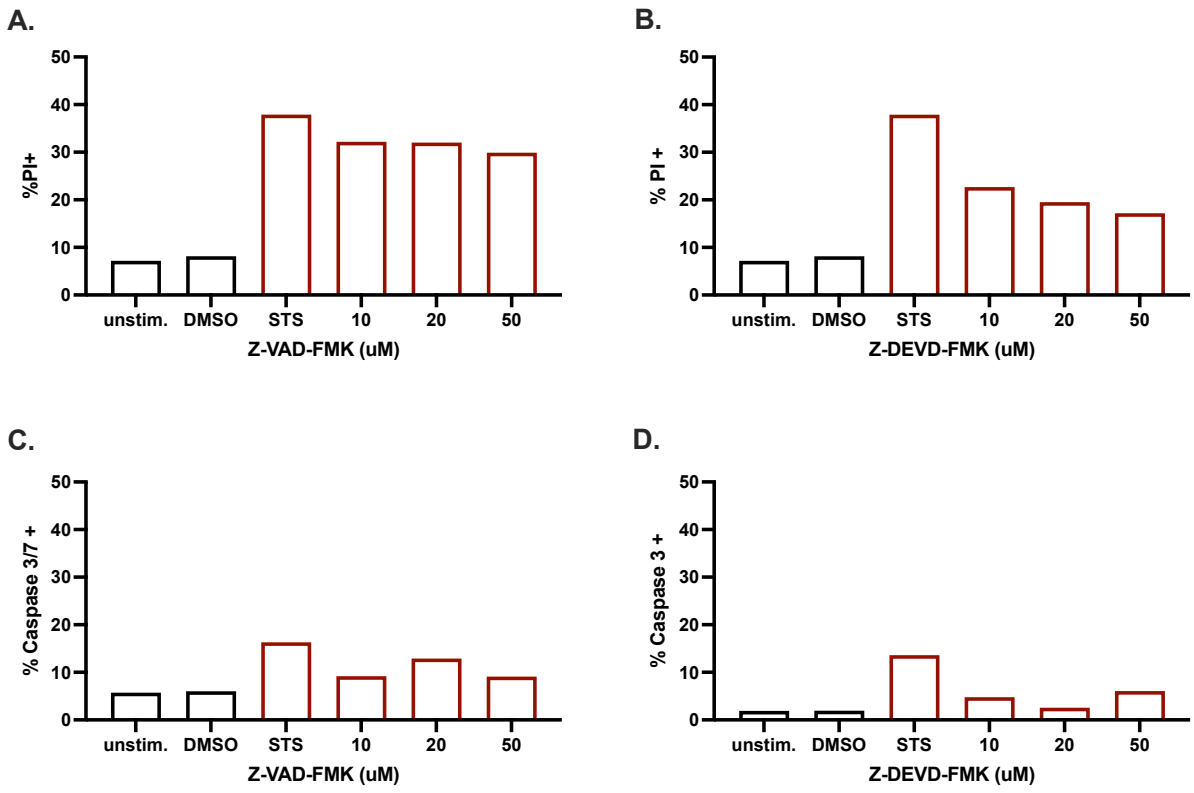

Supplementary Figure 7. Z- VAD-FMK and Z-DEVD-FMK optimizations on J1.1 cells. Cells were pre – treated for 1 hour with 10, 20, 50uM of either inhibitor, or left unstimulated. DMSO was used as a vehicle control. After 1 hour, 10uM Staurosporine was added to induce apoptosis. Following a 24-hour incubation, cells were stained with either PI (**A, B**), FLICA 660 caspase 3/7 stain (**C**), or an anti – active caspase 3 APC conjugated antibody (BD Biosciences # 560626, **D**). Cell death or caspase activity was analyzed using flow cytometry. No statistics performed (n = 1).

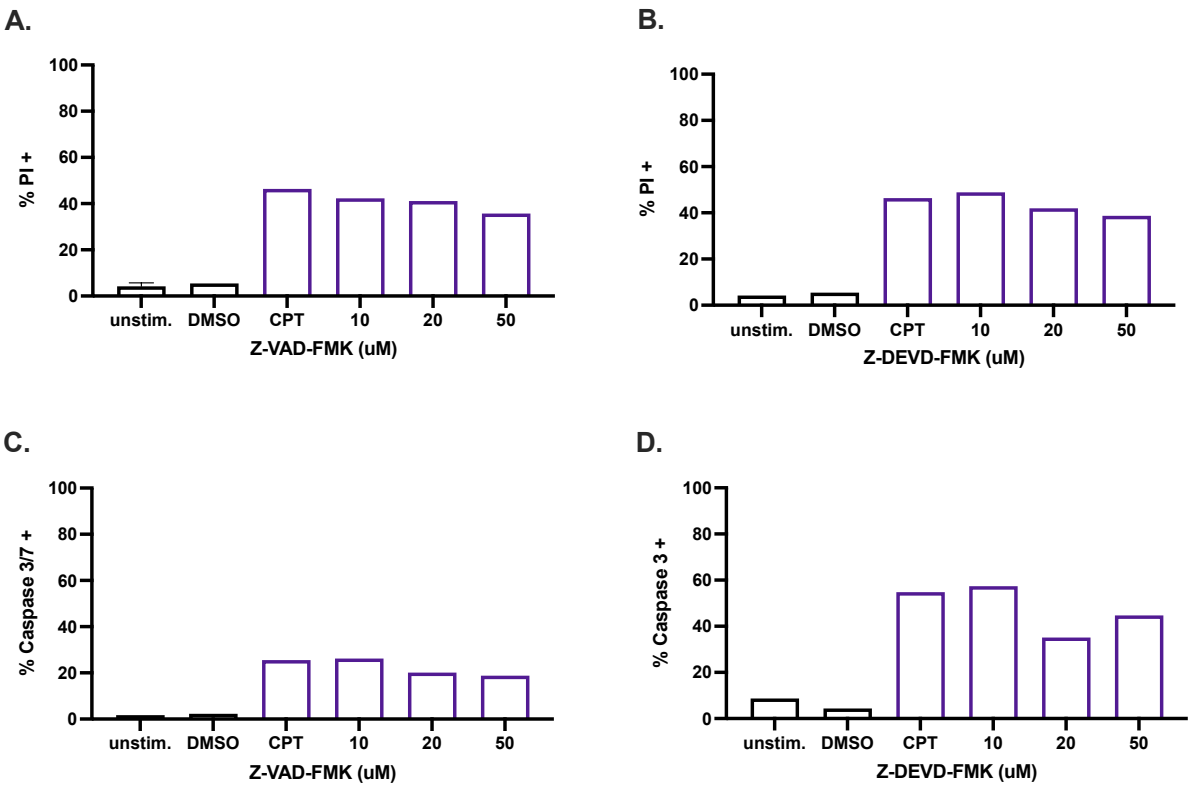

Supplementary Figure 8. Z- VAD-FMK and Z-DEVD-FMK optimizations on OM10.1 cells. Cells were pre – treated for 1 hour with 10, 20, 50uM of either inhibitor, or left unstimulated. DMSO was used as a vehicle control. After 1 hour, 0.2uM Camptothecin was added to induce apoptosis. Following a 24-hour incubation, cells were stained with either PI (**A, B**), FLICA 660 caspase 3/7 stain (**C**), or an anti – active caspase 3 APC conjugated antibody (BD Biosciences # 560626, **D**). Cell death or caspase activity was analyzed using flow cytometry. No statistics performed (n = 1).

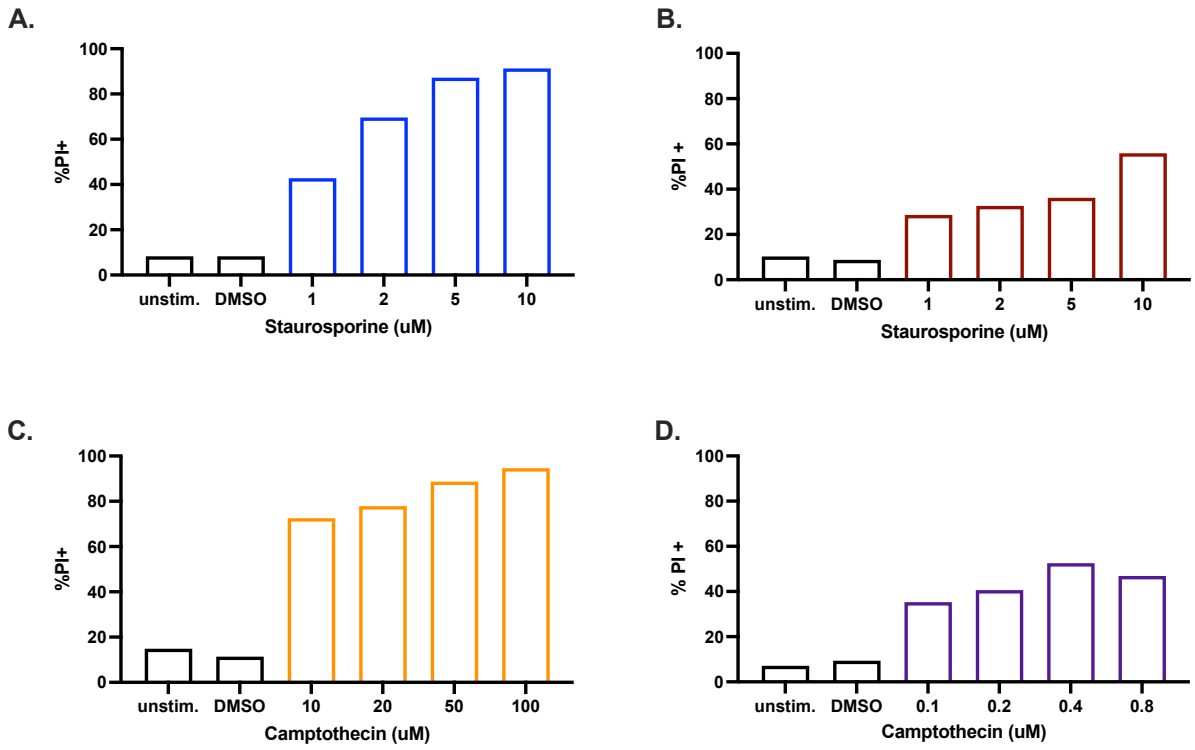

Supplementary Figure 9. Camptothecin/Staurosporine optimizations on Jurkat (A), J1.1 (B), U937 (C), and OM10.1 (D). Cells were treated with dose response concentrations of either Staurosporine or Camptothecin, left untreated, or treated with a DMSO vehicle control for 24 hours. Potency of each chemical cell death inducer was analyzed using flow cytometry staining for PI (i.e cell death). No statistics performed (n = 1).

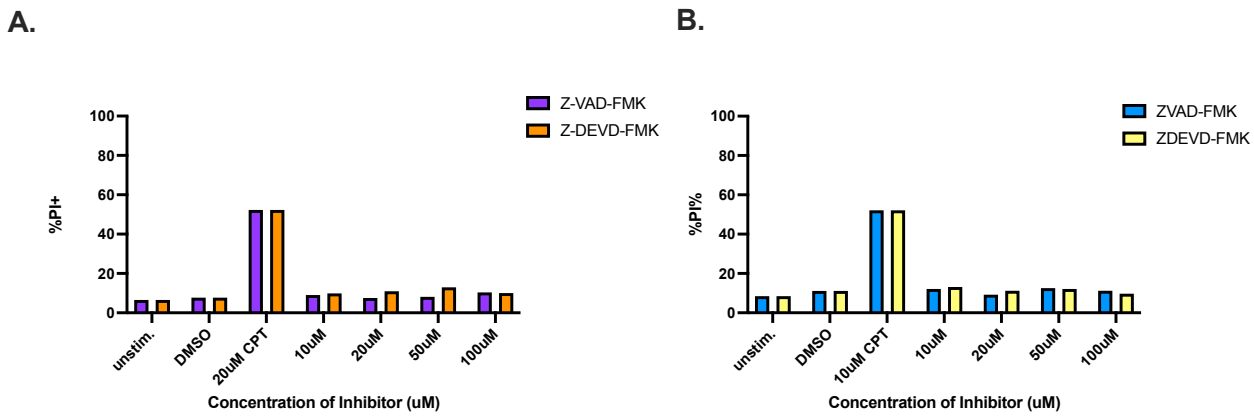

Supplementary Figure 10. Both Z-VAD-FMK and Z-DEVD-FMK are not cytotoxic and do not induce cell death in Jurkat (A) or U937 (B) cells. The effects of both caspase inhibitors on their own was investigated (i.e no cell death inducer present). Cells treated with 10 – 100uM of either inhibitor maintained similar levels of cell death to the unstimulated control, thus inhibitors do not cause any cytotoxicity's. Camptothecin was used as a positive control for apoptosis. Cells were treated for 24 hours, and cell death was analyzed on flow cytometry using Pi staining. No statistics performed (n = 1).

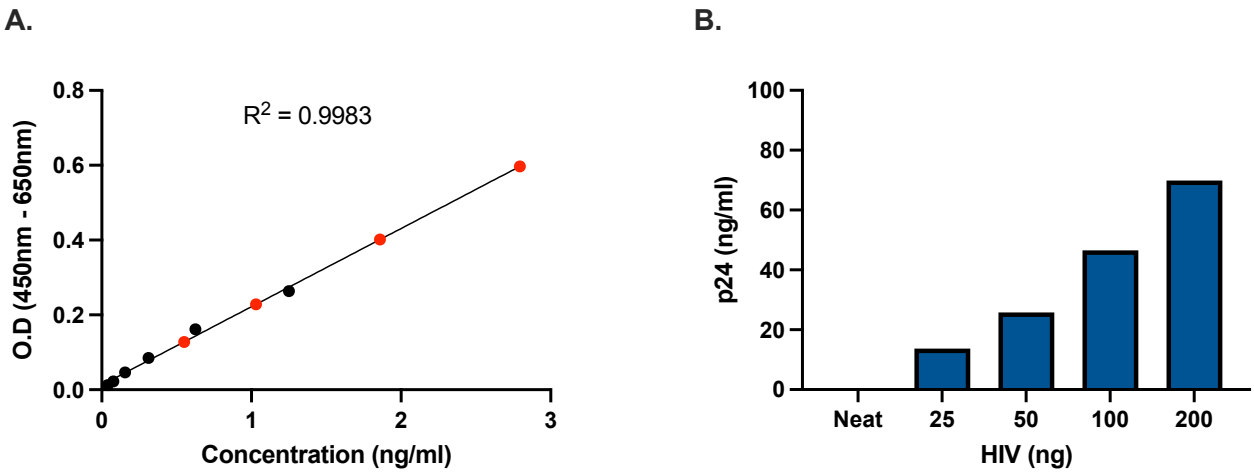

Supplementary figure 11. HIV p24 ELISA on MDM. MDM were infected with 25-200ng of HIV for 6 days. At 6.d.p.i, cell-free supernatants were lysed using Triton-X and p24 ELISA was performed. Concentration (ng/ml) of p24 was extrapolated from the standard curve (A), 100ng of HIV was chosen for future MDM infection experiments (B). Statistics not performed (n = 1).

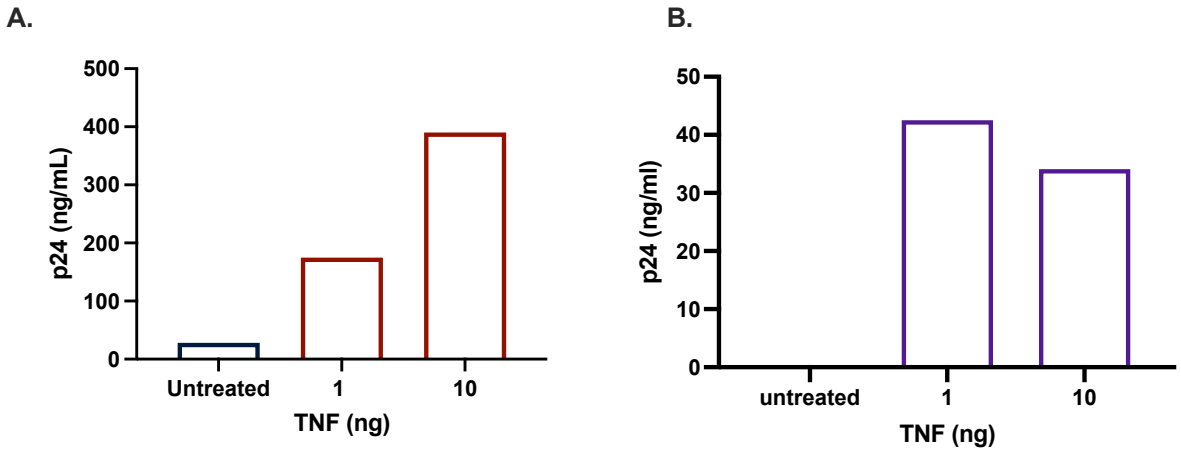

Supplementary Figure 12. HIV re – activation p24 ELISA on J1.1 (A) and OM10.1 (B) cells to confirm HIV latency. Cells were treated for 24 hours with 1 or 10ng or TNF-α to reactivate the latent reservoir. J1.1 cells (A) harbour slightly less of a true "latent" reservoir than OM10.1 cells, due to the production of HIV p24 capsid protein in the untreated control.

Other author contributions

Figure 4: One individual biological replicate on the OM10.1 cell line was completed by Angel lab PhD student Bengisu Moyler

Figure 5: Two individual biological replicates on the J1.1 cell line were completed by Angel lab PhD student Bengisu Moyler